# Generation of Mid-ocean Ridge Tholeiites*

*by* D. C. PRESNALL, J. R. DIXON, T. H. O'DONNELL†, *and* S. A. DIXON‡

*Department of Geosciences, The University of Texas at Dallas, P.O. Box 688, Richardson, Texas 75080*

(*Received 14 October 1977; in revised form 27 June 1978*)

## ABSTRACT

If a basaltic magma is separated from its mantle source region only after a large amount of fusion, as indicated for mid-ocean ridge tholeiites by large ion lithophile (LIL) element studies, volatile-free phase relationships may be used to model closely the fusion process at the site of origin. Volatile-free solidus curves in pressure–temperature space display low-temperature cusps where subsolidus phase transitions intersect the solidus, and these cusps are believed to be important in controlling the depth of magma generation and the compositions of primary magmas. In the system $CaO–MgO–Al_2O_3–SiO_2$, the solidus curve for simplified plagioclase and spinel lherzolite has been determined up to 20 kb, and a cusp has been found at 9 kb, 1300 °C, where the transition from simplified plagioclase to spinel lherzolite intersects the solidus and forms an invariant point. Simplified basaltic melts formed along the solidus curve change from quartz-normative compositions at low pressures to olivine-normative compositions at high pressures, and the composition of the first liquid produced at the 9 kb cusp resembles closely the composition of the least-fractionated mid-ocean ridge tholeiites. It is proposed that these least-fractionated basalts have been modified very little by fractional crystallization as they passed upward to the surface and are close to the composition of primary basalt generated at the mantle equivalent of the 9 kb cusp (30 km depth). Assuming a lherzolitic mantle source, the composition of this primary magma would be expected to remain fairly constant despite varying amounts of fusion as long as these amounts are between about 2 and 35 per cent, and despite variations in the proportions of minerals in the source region. For complex natural compositions in the mantle, the cusp would not be a point but would be expected to appear as a low temperature region on the solidus extending over a small pressure range at about 9 kb and 1200–1250 °C. It is suggested that magma generation at the cusp causes a sharp change in the slope of the geotherm beneath active ridges from approximately adiabatic at depths greater than about 30 km to strongly superadiabatic at depths less than 30 km. LIL element concentrations indicate that a close approach to fractional fusion is not applicable to the generation of primary magmas at spreading centers. Instead, a model involving varying amounts of equilibrium fusion is preferred, with fresh mantle being continually supplied at the 9 kb cusp as mantle material convects upward along the rising limb of a mantle convection cell. Primary magmas would thus be produced with fairly uniform major element compositions but widely different LIL element concentrations. Subsequent fractional crystallization of the primary magmas would produce most of the observed major element variations in the erupted basalts but would have only a second-order effect on the LIL element concentrations.

## INTRODUCTION

ONE of the most fundamental and elusive problems in igneous petrology is the determination of the nature of primary magmas (Presnall, in press) produced from the mantle and the processes responsible for their formation. It has been shown experimentally that the composition of a primary magma is dependent on a variety of parameters such as the depth and extent of melting (Yoder & Tilley, 1962; Green & Ringwood, 1967*a*; Kushiro, 1968) and the activities of $H_2O$, and $CO_2$ (Mysen & Boettcher, 1975). From these studies, it is clear that a completely

* Department of Geosciences, The University of Texas at Dallas, Contribution No. 345.

† Present address: U.S. Geological Survey, 307 Federal Building, Ft. Myers, Florida 33901.

‡ Mobil Research and Development Corp., Field Research Laboratory, Dallas, Texas 75221.

gradational series of compositionally diverse primary basalt magmas can be generated simply by varying these parameters. However, it does not necessarily follow that in nature each parameter is free to vary arbitrarily. In particular, the chemical coherence of major elements in tholeiites erupted at mid-ocean ridges seems to require a mechanism for producing enormous volumes of chemically homogeneous magma over long periods of time and on a global scale extending along the entire 65,000 km length of the worldwide ridge system. The purpose of this paper is to propose such a mechanism.

In any discussion of the generation of primary basalt magmas, the region of intersection of the mantle solidus and the geotherm is of obvious importance. Because the nature of this intersection depends on the shape of the solidus, some general features of solidus curves will be discussed first. Then, assuming lherzolite is the mantle source material for basalts, the solidus curve for simplified lherzolite in the system $CaO–MgO–Al_2O_3–SiO_2$ will be presented together with data on the compositions of first liquids produced along this curve and with diagrams showing the changing liquidus phase relations as a function of pressure. Finally, these phase relations will be used to model the generation of tholeiites at mid-ocean ridges.

## EFFECT OF VOLATILES ON MELTING RELATIONSHIPS

In this paper, attention will be directed primarily to volatile-free melting relationships. However, it is necessary first to discuss the effects of $H_2O$ and $CO_2$, because these components strongly affect not only the shape of the mantle solidus but also the compositions of initial melts.

First consider water. In the absence of any hydrous minerals, the solidus for a hydrous mantle will be the same regardless of the amount of water present, and at high pressures, this water-saturated solidus will be as much as several hundred degrees below the anhydrous solidus. The initial melts are also strongly enriched in silica relative to initial melts derived from corresponding anhydrous compositions (Kushiro, Yoder & Nishikawa, 1968; Kushiro, 1972*a*). If one or more hydrous minerals are stable, the solidus could be water-undersaturated, but it would still be possible for the temperatures and compositions of initial melts along this curve to be significantly enriched in silica relative to the anhydrous case.

It is commonly assumed that the mantle contains a small amount of water, but strong evidence has recently been presented that this assumption may be wrong for those regions of the mantle that yield mid-ocean ridge tholeiites. Delaney *et al.* (in press) have found that the water content of glass-vapor inclusions in olivine and plagioclase phenocrysts from mid-ocean ridge basalts is less than 0·002 wt. per cent. The glass in these inclusions is basaltic and similar in composition to the matrix glass surrounding the phenocrysts (O'Donnell, 1974). the matrix glass was found to contain 0·12 to 0·24 wt. per cent $H_2O$, and Delaney *et al.* concluded that this water entered the magma after formation of the phenocrysts. Barring some analytical problem or a mechanism, as yet unrecognized, for removing virtually all dissolved water soon after the magma is produced in the mantle, it would seem that the source region was essentially anhydrous; otherwise, the water would have been

concentrated in the melt. Thus, explanations for the origin of mid-ocean ridge tholeiites that involve hydrous fusion processes (Kushiro, 1973) are apparently not applicable.

Even if the above conclusions are rejected and the water found in the matrix glass of fresh mid-ocean ridge basalts is assumed to be derived from the mantle, the amount of $H_2O^+$, 0·1–0·5 wt. per cent (Hart & Nalwalk, 1970; Moore, 1970; Bryan & Moore, 1977), is a factor of 20–100 below that required to produce saturation (Hamilton *et al.*, 1964) at the depth of origin of the magma, assuming this depth to be 25–30 km (Green & Ringwood, 1967*a*; Kay *et al.*, 1970). For such small amounts of water, anhydrous melting relationships are an excellent approximation of the actual melting relationships if the amounts of fusion are large. That is, melts may be produced at very low temperatures for a mantle containing a small amount of water, but if these melts are separated from the source region only after a large amount of fusion such that the $H_2O$ content of the melt drops to 0·1–0·5 wt. per cent, the temperature and composition of the melt will be very close to that of the corresponding melt at the anhydrous solidus. For mid-ocean ridge tholeiites, a large amount of melting, 10–30 per cent, is strongly supported by data on concentrations of large ion lithophile (LIL) elements (Gast, 1968; Kay *et al.*, 1970; Schilling, 1971, 1975), and it appears safe to use anhydrous melting relationships as a close approximation of the actual melting relationships.

At pressures below about 25 kb, carbon dioxide is much less soluble in silicate melts than water. The $CO_2$-saturated solidus is only slightly depressed below the anhydrous solidus, and the compositions of initial melts are shifted toward more alkalic compositions (Eggler, 1974, 1975, 1976; Wyllie & Huang, 1975; Mysen & Boettcher, 1975). In their studies of mid-ocean ridge basalts, Delaney *et al.* (in press) found 0·2–0·4 wt. per cent $CO_2$ in glass-vapor inclusions in olivine and plagioclase phenocrysts, and considered that the amount of $CO_2$ in the inclusions may be greater than that in the magma at the time of formation of the inclusions (see also Roedder, 1965, p. 1772). Thus, these data support the existence of only a small amount of $CO_2$ in the mantle source region and the arguments used above for water would apply for $CO_2$ as well. That is, for large amounts of fusion, $CO_2$-free melting relationships would closely approximate the actual melting relationships.

On the other hand, melting relationships in the presence of $CO_2$ and possibly $H_2O$ may be very important in explaining the low-velocity zone (Lambert & Wyllie, 1970*a*, 1970*b*; Wyllie & Huang, 1975; Eggler, 1976). In this case, only very small amounts of melting are required and the vapor-saturated solidus becomes important. However, the existence of a seismic low-velocity zone produced by very small amounts of melting and the production of basaltic magmas that rise to the earth's surface need not necessarily be related in any simple way. Thus, despite the fact that the importance of $CO_2$ and $H_2O$ in generating different types of basalts has recently been emphasized (Mysen & Boettcher, 1975), the effects of these constituents on the generation of mid-ocean ridge tholeiites are considered here to be very small. For these rocks, melting relationships in the absence of volatiles will be treated as a close approximation of the actual melting relationships.

## VOLATILE-FREE SOLIDUS CURVES

Volatile-free pressure–temperature solidus curves for mantle materials frequently are drawn with a continuously positive slope and either as straight lines or with only a slight curvature. In detail, such curves cannot be correct. To illustrate this point, the pressure–temperature isopleth for the composition 50 per cent albite, 50 per cent jadeite by weight in the binary system $NaAlSiO_4$–$SiO_2$ is shown in Fig. 1, based on the diagrams of Bell & Roseboom (1969). Although such a composition is not a good approximation of the mantle, the system has been carefully studied and is useful for illustrating principles. The solidus curve, drawn as a heavy solid line, shows three discontinuities or cusps at $i_1$, $i_2$, and $i_3$, and a variety of slopes, both positive and negative. Each cusp coincides with an invariant point produced by the intersection of the solidus with a subsolidus univariant reaction. For a geotherm that gradually rises and comes into grazing incidence with this solidus curve in the pressure range 20–40 kb, melting would be expected first at the cusp $i_1$, and this cusp would determine the depth of melting and control the composition of the primary magma. It will be argued later that a similar cusp on the mantle solidus determines the depth of origin and controls the composition of primary magmas generated at mid-ocean ridges.

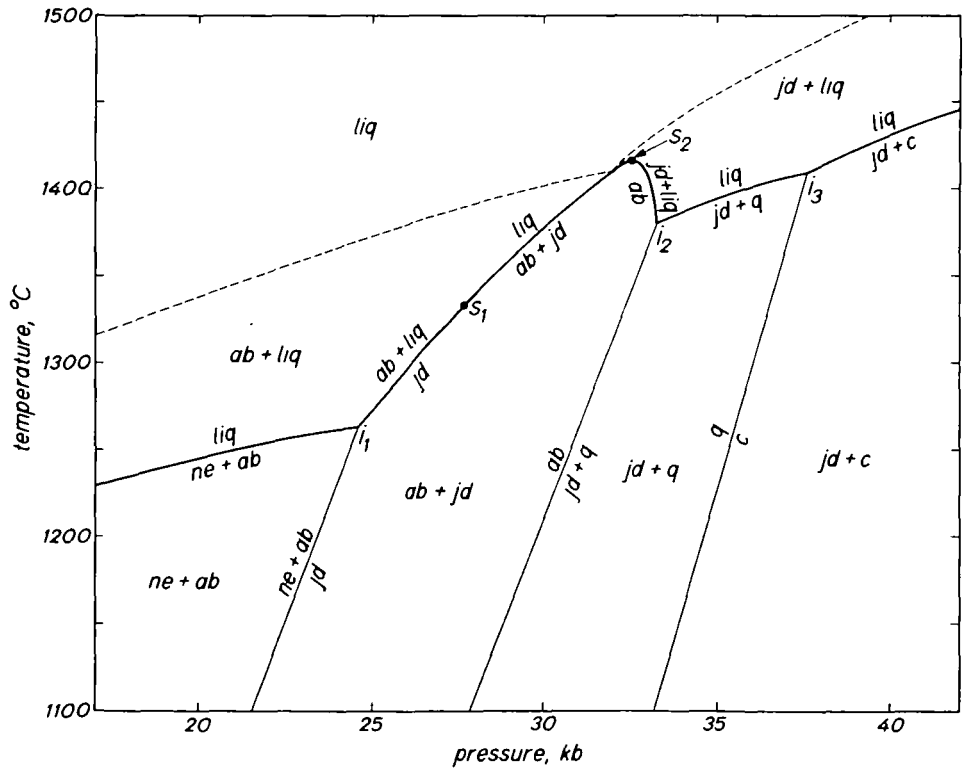


FIG. 1. Pressure–temperature isopleth for the composition 50 per cent albite, 50 per cent jadeite by weight in the system $NaAlSiO_4$–$SiO_2$, based on the diagrams of Bell & Roseboom (1969). All solid lines are univariant reactions, $i_1$, $i_2$, and $i_3$ are invariant points, and $s_1$ and $s_2$ are singular points. The dashed liquidus curve is not univariant. *ab* = albite, *ne* = nepheline, *jd* = jadeite, *q* = quartz, *c* = coesite, *liq* = liquid.

The lack of irregularities in the slopes of previously studied solidus curves for complex compositions such as pyrolite (Green & Ringwood, 1967*b*) could be caused by several factors: (1) Irregularities on solidus curves for complex multicomponent compositions may be minor and not easily detected. From theoretical considerations, it is evident that irregularities must exist in any system showing subsolidus phase transitions that intersect the solidus, but there is no requirement that these irregularities be large. (2) The experimental determination of the solidus is difficult in many cases because of problems in detecting very small amounts of glass in the run-products. (3) Experiments may be spaced too far apart. For example, in Fig. 1, if the solidus were determined only at 20, 27, 33, and 40 kb, most of the interesting complications would be missed and a nearly straight line could be drawn through the data points.

## SOLIDUS CURVE FOR MODEL LHERZOLITE IN THE SYSTEM $CaO–MgO–Al_2O_3–SiO_2$

For a lherzolitic upper mantle, major subsolidus phase transitions intersect the solidus at about 9 kb where plagioclase lherzolite (olivine + enstatite + diopside + plagioclase) transforms to spinel lherzolite (olivine + enstatite + diopside + spinel) (Kushiro & Yoder, 1966; Green & Hibberson, 1970; Emslie, 1971; Herzberg, 1972; Herzberg & O'Hara, 1972; Presnall, 1976) and about 23–30 kb where spinel lherzolite transforms to garnet lherzolite (olivine + enstatite + diopside + garnet) (MacGregor, 1965; Kushiro & Yoder, 1965, 1966; Green & Ringwood, 1967*b*; O'Hara *et al.*, 1971). To test the possibility that these transitions produce prominent low-temperature cusps on the mantle solidus, we have studied the solidus curve for simplified lherzolite in the system $CaO–MgO–Al_2O_3–SiO_2$ (Fig. 2). This system was chosen as a model of the mantle because it includes all three lherzolite mineral assemblages and accounts for about 90 per cent of the composition of the mantle, yet contains sufficiently few components that compositions of phases can be represented geometrically in a tetrahedron.

At present, we have studied the simplified lherzolite solidus up to 20 kb, and thus have examined only the invariant point defining the intersection of the solidus and the plagioclase to spinel lherzolite transition curve. The higher pressure invariant point defining the intersection of the solidus with the spinel to garnet lherzolite transition curve has not yet been determined.

Fig. 3, based on data in Table 1, shows the solidus curve from 1 atm to 20 kb. A cusp at 9 kb, 1300 °C separates the solidus into two parts, one being the univariant line (*sp*) that defines the solidus for the assemblage *fo* + *en* + *di* + *an* from 1 atm to 9 kb, and the other being the univariant line (*an*) that defines the solidus for the assemblage *fo* + *en* + *di* + *sp* above 9 kb. The position of curve (*liq*), based on the solidus intersection at 9 kb determined here and the slope determined by Kushiro & Yoder (1966), is consistent with all of the data presently available for this curve (Kushiro & Yoder, 1966; Green & Hibberson, 1970; Herzberg, 1972; Herzberg & O'Hara, 1972; Presnall, 1976). Presnall (1976) gave the position of the invariant point as 1305 °C, 9·0 kb. We have lowered the temperature 5° to make the revised solidus curves (*sp*) and (*an*) more consistent with our new data, but the new

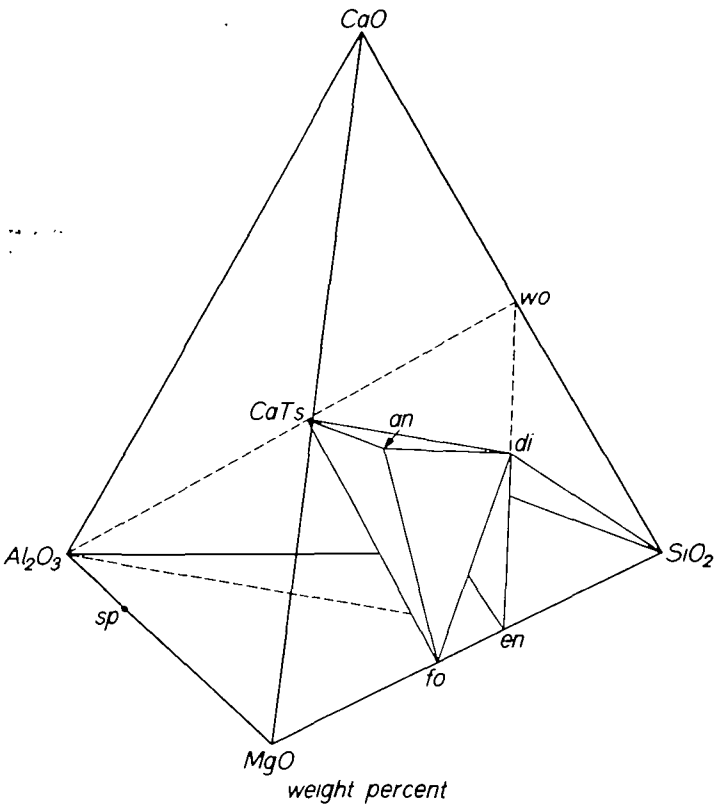


FIG. 2. The tetrahedron $CaO$–$MgO$–$Al_2O_3$–$SiO_2$ showing the simplified basalt tetrahedron *fo*–*di*–*CaTs*–$SiO_2$. The plane of aluminous pyroxene compositions is dashed. *CaTs* = Ca Tschermak's molecule ($CaAl_2SiO_6$), *wo* = wollastonite ($CaSiO_3$), *an* = anorthite ($CaAl_2Si_2O_8$), *di* = diopside ($CaMgSi_2O_6$), *sp* = spinel ($MgAl_2O_4$), *fo* = forsterite ($Mg_2SiO_4$), *en* = enstatite ($MgSiO_3$).

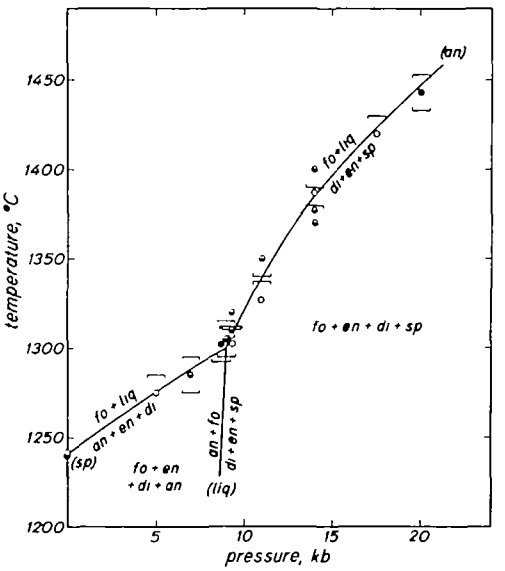


FIG. 3. Solidus curve for simplified plagioclase lherzolite (*fo* + *en* + *di* + *an*) and spinel lherzolite (*fo* + *en* + *di* + *sp*) in the system CaO–MgO–$Al_2O_3$–$SiO_2$. Phases in parentheses label the univariant curves according to the absent phase. Open circles are above the curve, half-filled circles are on the curve, and filled circles are below the curve. Brackets indicate experimental uncertainty. Some of the data points are from Presnall (1976). Abbreviations are as in Fig. 2.

TABLE 1

*Quenching experiments*

| *Mixture* | *Run No.* | *T*† (°C) | *P* (*kbar*) | *Time* (*hrs*) | *Phases present*‡ |
|---|---|---|---|---|---|
| CMAS-3 | 11 | 1240 | 1 atm | 73 | *fo* + *en** + *di** + *an* |
| CMAS-3 | 9 | 1242 | 1 atm | 48 | *gl* + *fo* + *en** + *di** + *an* |
| CMAS-7 | 122-6 | 1275 | 5 | 48 | *gl* + *fo* + *an* |
| CMAS-7 | 122-9 | 1285 | 7 | 48 | *gl* + *fo* + *en** + *di** + *an** |
| CMAS-5 | 122-1 | 1302 | 9·3 | 48 | *gl* + *fo* + *px* + *sp* |
| CMAS-5 | 121-5 | 1307 | 9·3 | 51 | *gl* + *fo* + *di** + *sp* |
| CMAS-5 | 122-8 | 1327 | 11 | 48 | *gl* + *fo* + *en** + *q*(*px*) |
| CMAS-6 | 124-2 | 1370 | 14 | 48 | *gl* + *fo* + *en** + *di** + *sp* + *q*(*px*,*fo*) |
| CMAS-6 | 122-3 | 1377 | 14 | 48 | *gl* + *fo* + *en** + *di** + *sp* + *q*(*px*,*fo*) |
| CMAS-6 | 122-2 | 1387 | 14 | 50 | *gl* + *fo* + *en** + *sp* + *q*(*px*,*fo*) |
| CMAS-6 | FEDS-13 | 1420 | 17·5 | 51 | *gl* + *fo* + *en** + *sp* + *q*(*px*,*fo*) |
| CMAS-6 | FEDS-12 | 1443 | 20 | 51 | *gl* + *fo* + *en** + *di** + *sp* + *q*(*px*) |

† W3Re/W25Re thermocouple for high pressure runs, Pt/Pt10Rh thermocouple for 1 atm runs.

‡ *fo*—forsterite, *en*—enstatite, *di*—diopside, *px*—pyroxene (diopside or enstatite or both), *an*—anorthite, *sp*—spinel, *gl*—glass, *q*—quench crystals with the type of quench crystals indicated in parentheses.

* Phase identification verified by electron microprobe.

positions of the invariant point and solidus curve are still within the uncertainty of the earlier data. A cusp is theoretically required at the invariant point (Schreinemakers, 1915*a*, *b*, *c*), and the experimental results agree with the required arrangement of univariant lines. Three other univariant lines originating from the invariant point have not been studied and are omitted.

TABLE 2

*Electron microprobe analyses of glasses*

| *Run No.** | *9* | *122-9* | *116-5*† | *116-3*‡ | *124-2* | *FEDS-12* |
|---|---|---|---|---|---|---|
| *Pressure* | *1 atm* | *7 kb* | *9·3 kb* | *11 kb* | *14 kb* | *20 kb* |
| *Spots analyzed* | *4* | *8* | *4* | *9* | *7* | *8* |
| $SiO_2$ | 55·79 ± 0·37** | 49·82 ± 0·18 | 48·85 ± 0·63 | 48·60 ± 0·37 | 48·30 ± 0·43 | 47·47 ± 0·21 |
| $Al_2O_3$ | 15·43 ± 0·21 | 18·65 ± 0·21 | 20·24 ± 0·28 | 19·51 ± 0·33 | 18·23 ± 0·25 | 17·19 ± 0·32 |
| MgO | 12·02 ± 0·20 | 14·43 ± 0·25 | 14·09 ± 0·37 | 15·52 ± 0·41 | 17·26 ± 0·47 | 19·90 ± 0·24 |
| CaO | 15·52 ± 0·37 | 15·51 ± 0·03 | 15·36 ± 0·04 | 15·30 ± 0·12 | 15·02 ± 0·19 | 13·86 ± 0·12 |
| TOTAL | 98·76 | 98·41 | 98·54 | 98·93 | 98·81 | 98·42 |
| | | | *CIPW norms (weight per cent)* | | | |
| *q* | 12·33 | 0·72 | — | — | — | — |
| *an* | 42·65 | 51·72 | 56·05 | 53·81 | 50·34 | 47·66 |
| *di* | 27·47 | 20·59 | 16·57 | 17·84 | 19·51 | 17·28 |
| *en* | 17·55 | 26·98 | 26·11 | 22·62 | 20·04 | 18·02 |
| *fo* | — | — | 1·27 | 5·74 | 10·11 | 17·05 |

* Run numbers keyed to Table 1, except for 116-5 and 116-3.

** Standard deviation.

† Mixture CMAS-5, 1310 °C, 24 hrs, *ol* + *en* + *di* + *sp* + *gl*, both pyroxenes verified by electron microprobe (see Presnall, 1976, table 3).

‡ Mixture CMAS-5, 1350 °C, 24 hrs, *ol* + *en* + *di* + *sp* + *gl*, both pyroxenes verified by electron microprobe (see Presnall, 1976, table 3).

## COMPOSITIONS OF LIQUIDS ALONG THE SOLIDUS

Just as the composition and mineralogy of the mantle are closely approximated by the system $CaO–MgO–Al_2O_3–SiO_2$, so also are the composition and mineralogy of tholeiites. The components CaO, MgO, $Al_2O_3$, and $SiO_2$ make up 80–88 per cent of the composition of tholeiites, and representatives (forstèrite, enstatite, diopside, anorthite, spinel, and quartz) of all the important phases found in these basalts are included.

Compositions of liquids along the solidus of Fig. 3, given in Table 2, are initial melt compositions for simplified plagioclase and spinel lherzolites. These liquids are basaltic in a simplified sense, and in order to see how their compositions change with pressure, the tetrahedron *fo–di–an–*$SiO_2$ has been used (Fig. 2). This small tetrahedron within the larger tetrahedron $CaO–MgO–Al_2O_3–SiO_2$ is a simplified version of the tholeiitic portion of the basalt tetrahedron, olivine–diopside–plagioclase–quartz (Yoder & Tilley, 1962). Three projections have been constructed. One is from *di* onto the base of the tholeiitic basalt tetrahedron, *fo—an—*$SiO_2$ (Fig. 4), another is from *an* onto the right front face, *fo–di–*$SiO_2$ (Fig. 5), and the third is from $SiO_2$ onto the left front face *di–fo–an* (Fig. 6). Kushiro (1972*c*) previously determined the composition of the liquid in equilibrium with forsterite, enstatite, diopside, and spinel in the system $CaO–MgO–Al_2O_3–SiO_2$ at 10 kb, and for comparison, this composition is shown in each projection. His run was at 1350 °C whereas we find the solidus at 10 kb to be at 1315 °C. The reason for the temperature and compositional discrepancy with Kushiro's result is not clear.

Previous work has established in only a very general way that as pressure increases, the first liquids produced by partial fusion of mantle compositions move

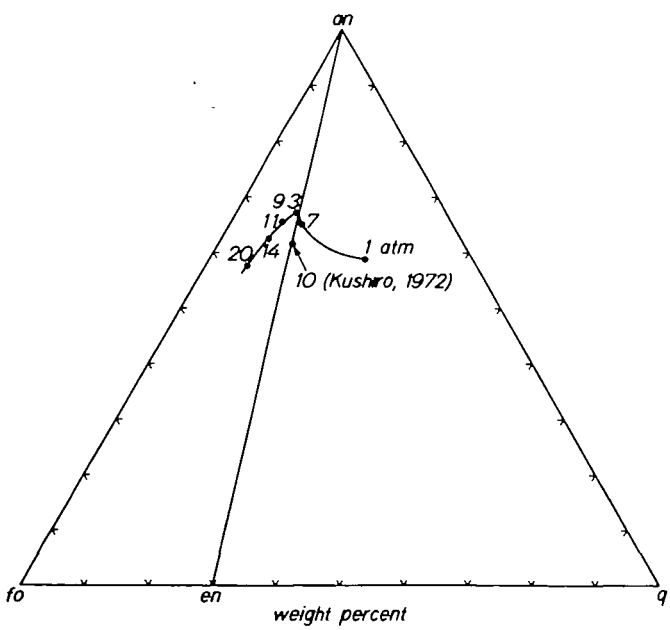


FIG. 4. Projection from *di* showing compositions of liquids along the solidus curve in Fig. 3. Numbers indicate pressures in kilobars. Abbreviations are as in Fig. 2.

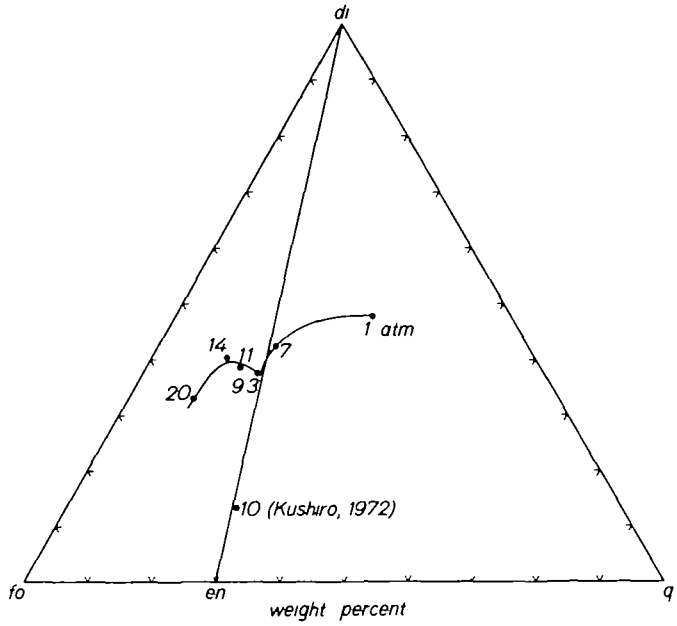


FIG. 5. Projection from *an*. For explanation, see caption to Fig. 4.

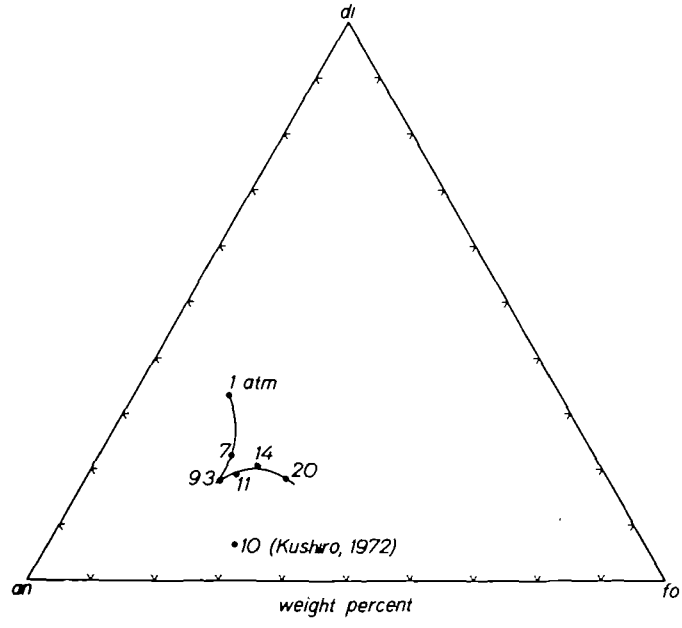


FIG 6. Projection from *q*. For explanation, see caption to Fig. 4.

from tholeiitic to alkalic compositions (Green & Ringwood, 1967*a*; Kushiro, 1968). Our data are in agreement with the direction of this trend and provide some additional details. From Figs. 4, 5, and 6, it can be seen that from 1 atm to 9 kb along the solidus for simplified plagioclase lherzolite, the first melting liquid

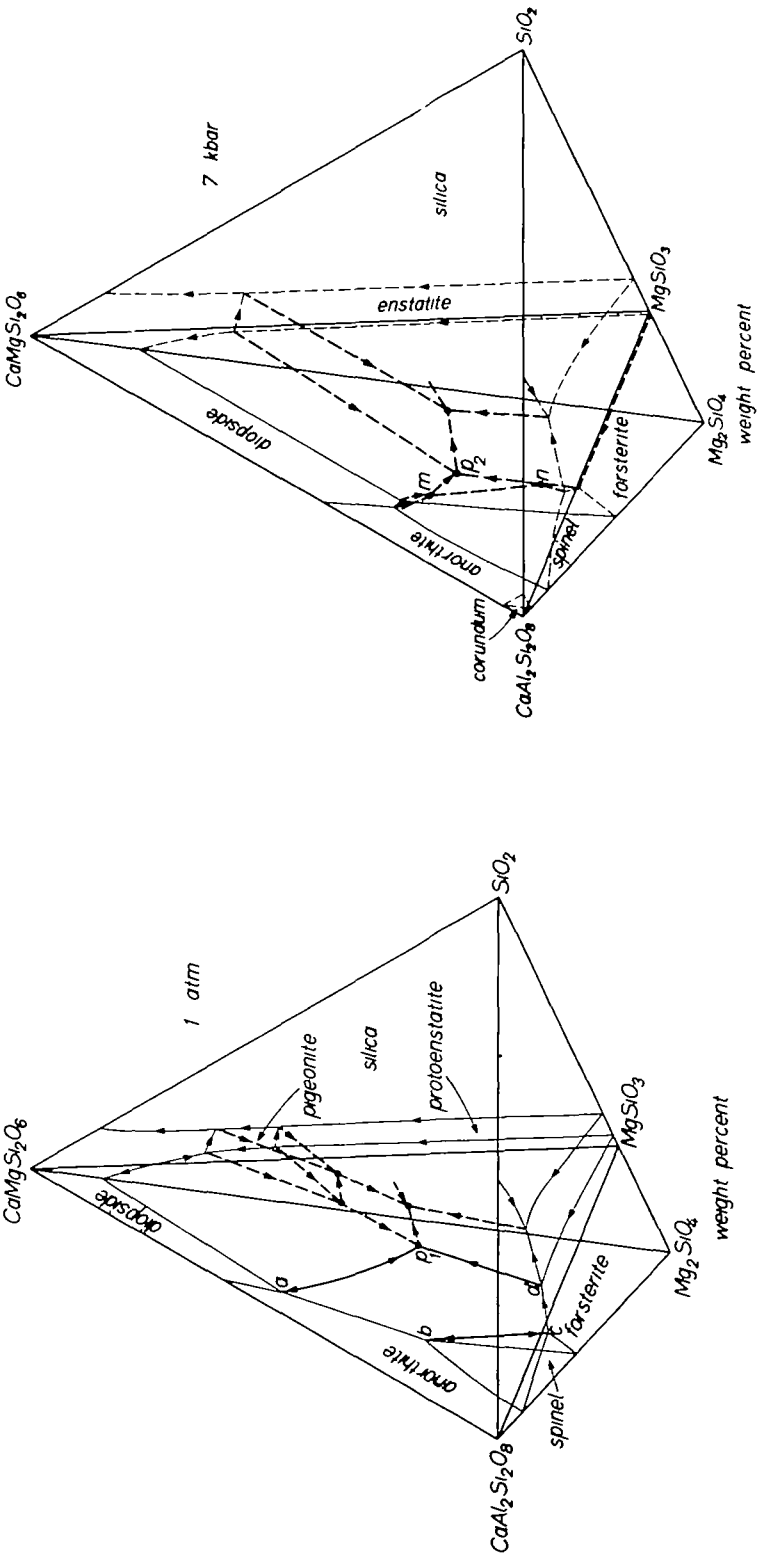


FIG. 7. Liquidus phase relations in the simplified tholeiitic basalt tetrahedron $Mg_2SiO_4$–$CaMgSi_2O_6$–$CaAl_2Si_2O_8$–$SiO_2$ at 1 atm. Heavy lines (dashed where inferred) with arrows indicating directions of decreasing temperature are liquidus univariant lines within the tetrahedron. Light lines (dashed where inferred) are intersections of quaternary divariant surfaces with the faces of the tetrahedron. Compiled from Osborn & Tait (1952), Bowen (1914), Andersen (1915), Kushiro (1972*b*), Hytönen & Schairer (1960), Yang (1973), and data in this paper. The back face, $CaMgSi_2O_6$–$CaAl_2Si_2O_8$–$SiO_2$, determined by Clark *et al.* (1962) is omitted for clarity.

FIG. 8. Liquidus phase relations in the tetrahedron $Mg_2SiO_4$–$CaMgSi_2O_6$–$CaAl_2Si_2O_8$–$SiO_2$ at 7 kb. Lines are as in Fig. 7. Compiled and interpolated from Kushiro (1969, 1972*b*), Presnall *et al.* (1978) and data in this paper.

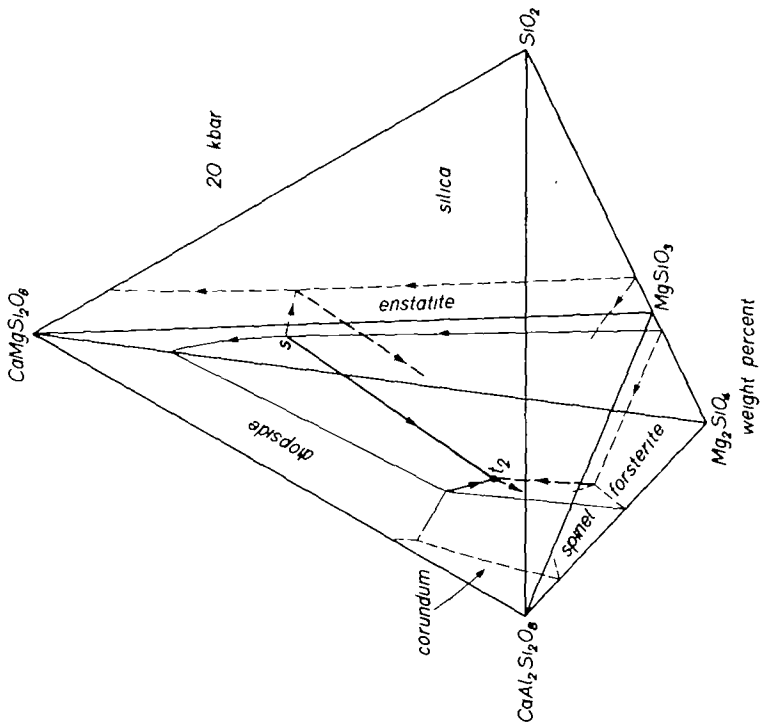


FIG. 9. Liquidus phase relations in the tetrahedron $Mg_2SiO_4$–$CaMgSi_2O_6$–$CaAl_2Si_2O_8$–$SiO_2$ at 10 kb. Lines are as in Fig. 7. Compiled and interpolated from Kushiro (1969, 1972*b*), Presnall *et al.* (1978) and data in this paper.

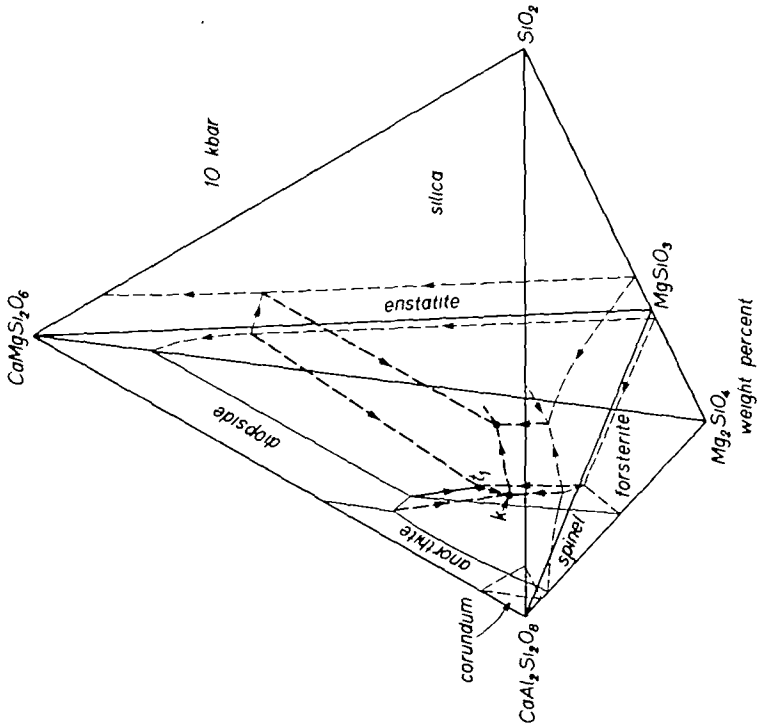


FIG. 10. Liquidus phase relations in the tetrahedron $Mg_2SiO_4$–$CaMgSi_2O_6$–$CaAl_2Si_2O_8$–$SiO_2$ at 20 kb. Lines are as in Fig. 7. Compiled from Kushiro (1969), Presnall *et al.* (1978), and data in this paper.

changes from a quartz tholeiite* to a composition just inside the olivine tholeiite volume. As pressure increases in this range, normative anorthite increases and normative diopside decreases. The discontinuity in the composition trend of the first-liquid compositions at 9 kb coincides with the 9 kb cusp in Fig. 3. From 9 kb up to the current limit of our data at 20 kb, the first liquid compositions become enriched in forsterite, depleted in anorthite and enstatite, and change very little in diopside content.

## LIQUIDUS PHASE RELATIONS IN THE SIMPLIFIED THOLEIITE TETRAHEDRON

By combining the data in Table 2 with other data in the literature, it is possible to construct approximate liquidus phase relations for the tholeiitic part of the simplified basalt tetrahedron at various pressures from 1 atm to 20 kb. Figs. 7 to 10 show the phase relations at 1 atm, 7 kb, 10 kb, and 20 kb. In these diagrams, the isobaric quaternary peritectics $p_1$, $p_1$, $t_1$, and $t_2$ correspond to liquid compositions along the solidus curve in Fig. 3. At pressures above 1 atm, these points constitute the only information that has been obtained on the positions of isobaric univariant lines and invariant points within the tetrahedra. The positions of the other isobaric quaternary invariant points shown in these figures are inferred.

As pressure increases from 1 atm, points *a* and *b* (Fig. 7) approach each other until, at about 5 kb, they touch as a result of the isobaric invariant point *m* (Fig. 8) passing into the tetrahedron through the left face (Presnall *et al.*, 1978). Similarly, points *c* and *d* (Fig. 7) approach each other as pressure increases, causing the isobaric invariant point *n* (Fig. 8) to move into the tetrahedron through the base. As pressure increases, the three isobaric invariant points *m*, *n*, and $p_2$ (Fig. 8) continue to converge, finally collapsing into a single point at the 9 kb invariant point in *P–T* space (Fig. 3). Further increase in pressure above 9 kb results in the appearance of two new isobaric invariant points, *k* and $t_1$ (Fig. 9). The points *m* and *n* in Fig. 8 and *k* in Fig. 9 each lie on one of the three univariant lines in *P–T* space omitted, for clarity, from Fig. 3.

## THE ALLEGED THERMAL DIVIDE BETWEEN QUARTZ NORMATIVE AND OLIVINE NORMATIVE BASALTS

It is not the main purpose of this paper to discuss the fractional crystallization of mid-ocean ridge basalts, but there is one important feature of Figs. 7 to 10 that will be mentioned briefly in this regard. O'Hara (1965, 1968*a*) proposed that the join enstatite–diopside–plagioclase becomes a thermal divide separating quartz-normative from olivine-normative tholeiites at pressures above 5 kb. Shibata (1975) suggested that this join becomes a thermal divide at pressures as low as 2–3 kb and proposed that the characteristic olivine-normative compositions of mid-ocean ridge tholeiites are due to fractional crystallization of an olivine-normative parent at 2–3 kb such that the fractionating liquids are trapped between the two

* The term quartz tholeiite will refer to compositions in the normative tetrahedron *hy–pl–di–q* (for natural basalts) or *en–an–di–q* (for simplified basaltic compositions). Similarly, the term olivine tholeiite will refer to compositions in the normative volume *hy–pl–di–ol* or *en–an–di–fo*.

thermal divides olivine–diopside–plagioclase and enstatite–diopside–plagioclase. Clague & Bunch (1976) pointed out, however, that many mid-ocean ridge basalts from the eastern Pacific are highly fractionated and quartz-normative. They argued that these basalts are derived from olivine-normative basalts and therefore must have been fractionated at a pressure less than 2–3 kb where no thermal divide exists.

O'Hara (1965) seems to have originally proposed the existence of the enstatite–diopside–plagioclase divide because enstatite begins to melt congruently at a very low pressure (Boyd *et al.*, 1964: Chen & Presnall, 1975). However, due to complexities involving the crystallization of aluminous pyroxenes and spinel at high pressures (Figs. 8 and 9), the enstatite thermal divide on the join $Mg_2SiO_4$–$SiO_2$ disappears in the more complex system, and it can be seen from Figs. 7 to 10 that the join enstatite–diopside–anorthite is not a thermal divide at any pressure in the range 1 atm to 20 kb. Thus, to the extent that the system CaO–MgO–$Al_2O_3$–$SiO_2$ applies to natural basalts, it can be stated that fractionating basaltic liquids are not trapped in the olivine tholeiite volume and fractionation to quartz-normative compositions is not restricted to pressures less than 2–3 kb.

## COMPOSITIONS OF COMPLETELY LIQUID MID-OCEAN RIDGE THOLEIITES

In order to compare the normative compositions of mid-ocean ridge basalts to phase relations in the tetrahedron *di–fo–an–SiO*$_2$, it is important to eliminate analyses of rocks that have been altered. In particular, the oxidation state of iron has a strong effect on the norm and is easily affected by alteration. Fig. 11 shows a plot of $FeO/Fe_2O_3$ versus total water content for 173 wet chemical analyses of mid-ocean ridge tholeiites, taken from the literature. As the water content increases, the iron becomes more oxidized, but increasing water content appears to affect the iron oxidation state only for values of $H_2O^- + H_2O^+$ greater than 0·8 per cent. On this basis, all analyses of basalts with total water greater than 0·8 per cent have been eliminated. In addition, only analyses that represent liquid compositions are desired, so the data set has been further restricted to those analyses of rocks with petrographic descriptions indicating that they are aphanitic or glassy. Finally, the data set has been limited to those rocks that have locality descriptions accurate enough to be sure that they were sampled from within the median rift of a ridge and not from a fracture zone. The final set of data consists of 20 analyses, taken from Miyashiro *et al.* (1969), Shido *et al.* (1971), and Melson & Thompson (1971).

In addition to these 20 wet chemical analyses, a set of 50 electron microprobe analyses of glassy margins of pillow basalts in the FAMOUS area has recently been published (Bryan & Moore, 1977). These analyses meet all of the criteria established above except that $FeO/Fe_2O_3$ was not determined. In order to use the Bryan and Moore data, we have averaged the $Fe^{2+}/(Fe^{2+} + Fe^{3+})$ values for the 20 wet chemical analyses (average = 0·86) and imposed this value on all of the Bryan and Moore data.

Melson *et al.* (1976) have reported an even larger set of analyses of abyssal basalt glasses, also determined by electron microprobe. They have tabulated analyses of over 900 samples, but we have used only those that are indicated to be

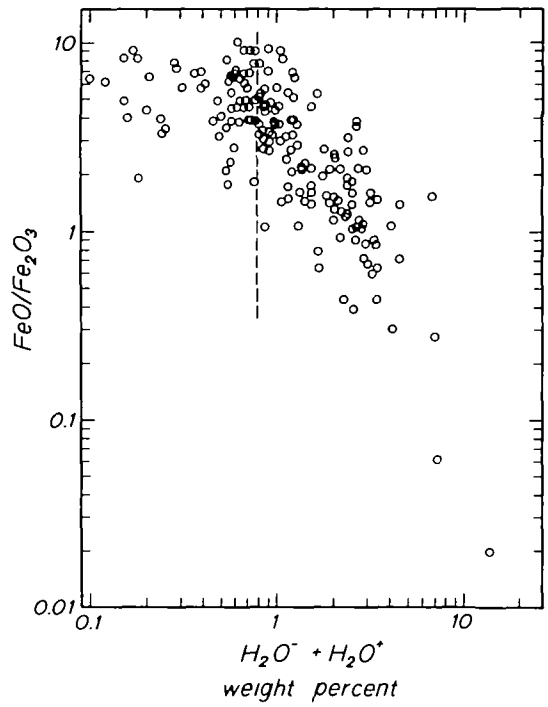


FIG. 11. $Fe_2O_3/FeO$ versus $H_2O^- + H_2O^+$ for 173 literature analyses of mid-ocean ridge tholeiites.

less than one million years old so as to be certain of including only the freshest material erupted from currently active ridges. Thus, 133 analyses from the Juan de Fuca Ridge and 208 analyses from the Galapagos spreading center have been retained. The ratio $Fe^{2+}/(Fe^{2+} + Fe^{3+})$ has been set at 0·86 for these basalts also.

In order to represent these basalt compositions, we have plotted normative diagrams as in Figs. 4, 5, and 6 except that normative albite has been retained with anorthite to form *pl*, fayalite with forsterite to form *ol*, hedenbergite with diopside to form *di*, and ferrosilite with enstatite to form *hy*. The sum of all of these normative constituents for the analyses plotted ranges from 87 to 99 wt. per cent. By including ferrosilite, an ambiguity is created in weight per cent plots like Figs. 4 and 5 because ferrosilite plots at a different location than enstatite. To avoid this problem, the norms have been plotted in terms of molecular proportions (Figs. 12, 13, and 14). Because of the large number of points, each of the groups of analyses is enclosed by a contour that contains 95 per cent of the analyses from that group.

Early workers who studied the compositions of abyssal tholeiites were impressed by the chemical homogeneity of these basalts (Engel & Engel, 1964; Engel *et al.*, 1965). This observation still has validity although it can be seen in Figs. 12, 13, and 14 that the data set is now large enough to reveal systematic chemical variations within samples from the same locality as well as differences among basalts from different areas. Most of the diversity within a given area is best explained by fractional crystallization (for example, see Miyashiro *et al.*, 1969; Shido *et al.*, 1971; Bryan & Moore, 1977). As will be discussed later, the least-fractionated basalts lie in the left-hand portion of the overall trend shown in Figs. 12 and 13,

with the extension to the right approximately toward the quartz apex being occupied by more fractionated basalts. For the less-fractionated basalts, there is extensive overlap of the compositions from both the Atlantic and Pacific ridges, with the most distinctive regional difference being the highly fractionated basalts from the Galapagos spreading center that are not duplicated elsewhere. However, care should be exercised when assigning importance to the distribution patterns shown. For example, analyses from the Galapagos spreading center are divided into two regions because most of the analyses came from only two sampling localities.

## COMPARISON WITH MELTING EXPERIMENTS ON COMPLEX COMPOSITIONS

Before the results from the present study are applied to mid-ocean ridge tholeiites, it is useful to examine the effects of additional components on phase

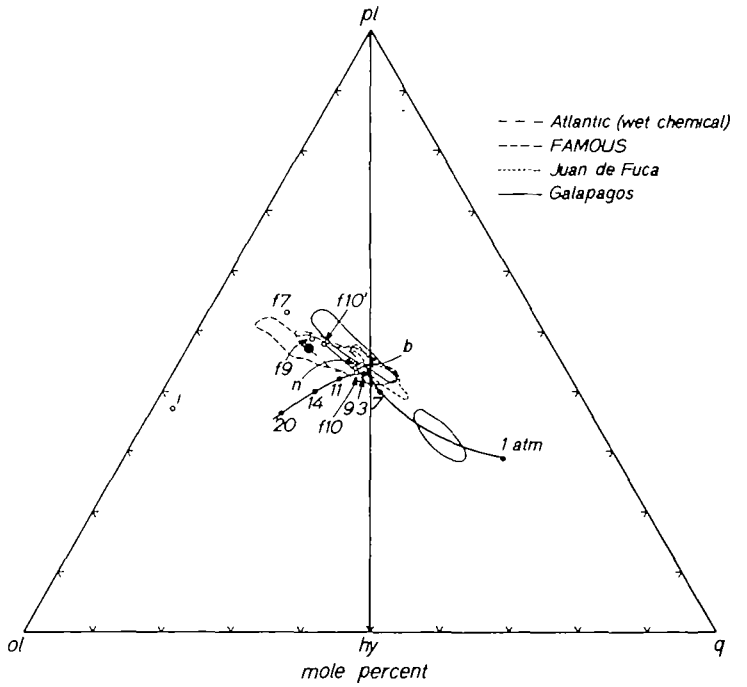


FIG. 12. Projection from *di* showing molecular CIPW norms of glassy and aphanitic mid-ocean ridge tholeiites and compositions of liquids along the solidus curve in Fig. 3. For each data set, the contour encloses 95 per cent of the analyses. Wet chemical analyses (20 analyses, all Atlantic) are from Miyashiro *et al.* (1969, analyses 3 to 15 inclusive, tables 3 and 4), Shido *et al.* (1971, analyses 17 to 21 inclusive, table 2), and Melson & Thompson (1971, analyses 2 and 3, table 3). The FAMOUS data (50 analyses) are from Bryan & Moore (1977). Data from the Galapagos spreading center (208 analyses) and the Juan de Fuca ridge (133 analyses) are from Melson *et al.* (1976). The large filled circle is the average Mt. Pluto magma from the FAMOUS area (Bryan & Moore, 1977). Point *b* is a glass formed by melting basalt T-87 at 7·5 kb (Kushiro, 1973, table 3). Point *n* is a glass in equilibrium with forsterite, orthopyroxene, clinopyroxene, and spinel at 10 kb in the system $Na_2O$–CaO–MgO–$Al_2O_3$–$SiO_2$ (Kushiro, 1972*c*, table 1). Points *f7*, *f9*, and *f10* are from Frey *et al.* (1964, table 3, analyses 7, 9, and 10). Point *f10'* is the same as *f10* with 0·4 per cent $Na_2O$ added. For all except the wet chemical analyses, $Fe^{2+}/(Fe^{2+} + Fe^{3+})$ has been set at 0·86. Numbers indicate pressures in kilobars. *ol* = $Mg_2SiO_4 + Fe_2SiO_4$, *hy* = $MgSiO_3 + FeSiO_3$, *di* = $CaMgSi_2O_6 + CaFeSi_2O_6$, *pl* = $CaAl_2Si_2O_8 + NaAlSi_3O_8$. *q* = $SiO_2$.

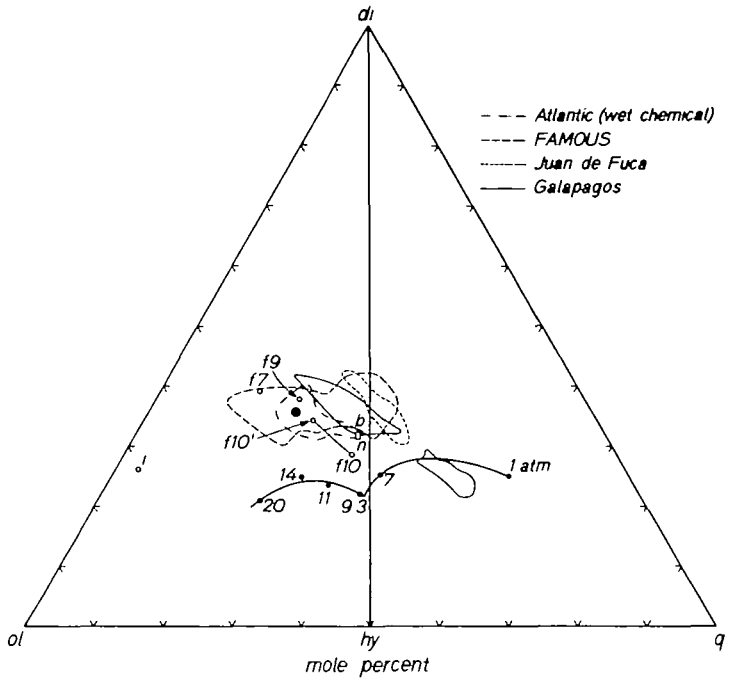


FIG. 13. Projection from *pl*. For explanation, see caption to Fig. 12.

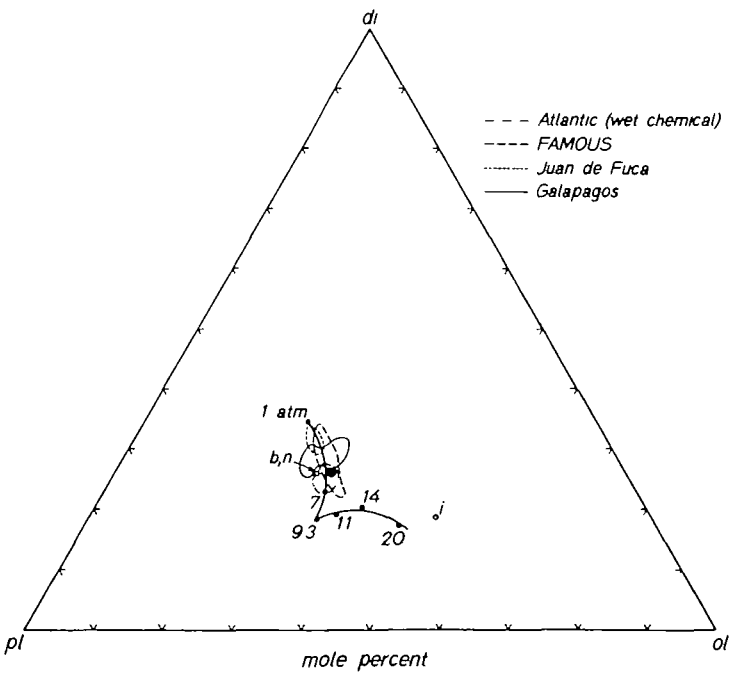


FIG. 14. Projection from *q*. For explanation, see caption to Fig. 12.

relations in the system $Ca–MgO–Al_2O_3–SiO_2$. It is impossible to discuss these effects with great precision, but some approximate changes to be expected are indicated by recent electron microprobe data on the compositions of liquids pro-

duced in partial melting experiments on natural lherzolites and basalts (Kushiro, 1973; Mysen & Kushiro, 1977) and in the system $Na_2O$–CaO–MgO–$Al_2O_3$–$SiO_2$ (Kushiro, 1972*c*).

In the system $Na_2O$–CaO–MgO–$Al_2O_3$–$SiO_2$ (Kushiro, 1972*c*), the composition of the liquid in equilibrium with olivine, orthopyroxene, clinopyroxene, and spinel at 10 kb (point *n* in Figs. 12, 13, 14) is decreased in normative *hy* and increased slightly in *pl*, *di*, and *ol*, relative to our composition at 10 kb without $Na_2O$. Kushiro's run is at 1325 °C, about the same as our temperature (1320 °C) for the solidus curve (Fig. 3). When $Na_2O$ is added, the temperature of runs showing liquid in equilibrium with olivine, enstatite, diopside, and spinel (an isobaric univariant line) should be lower than 1320 °C, but if temperature uncertainties in the apparatus are taken into account, his result may still be considered consistent with our data. However, at 20 kb, Kushiro analyzed a liquid in equilibrium with olivine, diopside, enstatite, and spinel at 1480 °C. Again, the temperature of such an assemblage should be below our solidus temperature at 20 kb, but in this case it is about 35° higher (Fig. 3), a difference that cannot be explained as experimental uncertainty. Using a small extrapolation of our solidus curve to higher pressures, the same problem exists with Kushiro's experiment at 25 kb. Consequently, we have not used his data at 20 and 25 kb.

Partial fusion experiments on natural lherzolites (Kushiro, 1973; Mysen & Kushiro, 1977) indicate that at pressures from 15 to 20 kb, liquid compositions are *ne*-normative for small amounts of partial fusion and change to *hy*-normative compositions as the amount of fusion increases. This change, which was also discussed by Green & Ringwood (1967*a*), is exactly what would be expected if the natural equivalent of point $t_2$ in Fig. 10 were shifted to the left of the plane $CaMgSi_2O_6$–$Mg_2SiO_4$–$CaAl_2Si_2O_8$ to an alkalic composition. Initial melts from a lherzolite source would then be alkalic. For amounts of fusion large enough to lose the isobaric invariant point control on the melt composition, and assuming spinel is the first phase to be completely dissolved, the liquid composition would move along the mantle equivalent of $t_2$–*s* towards *s* into the tholeiitic volume (see also Presnall *et al.*, 1978).

A final comparison can be made with the results of Kushiro (1973) on partial fusion of a mid-ocean ridge tholeiite (T-87) at 7·5 kb. The composition he found for the liquid in equilibrium with olivine, plagioclase, Ca-poor pyroxene, and Ca-rich pyroxene is plotted as point *b* in Figs. 12, 13, and 14. By changing the proportions of the phases, Kushiro's result could be considered comparable to a partial fusion experiment on a plagioclase lherzolite. In comparison to our first melt at 7·5 kb, it can be seen that the glass of the partially fused basalt is depleted in silica and enriched in *di* and *pl*.

From all of these comparisons taken together, it appears that the compositions of partial melts of natural lherzolites are depleted in silica and enriched in *di* and *pl* relative to our data in the system CaO–MgO–$Al_2O_3$–$SiO_2$. The depletion in $SiO_2$ is such that first liquids in more complex systems probably would become *ne*-normative at about 12 kb (Presnall *et al.*, 1978). It is probable that in the system CaO–MgO–$Al_2O_3$–$SiO_2$, first liquids produced from melting simplified lherzolite

do not lie on the silica-poor side of the plane *di–fo–an*, that is, in the simplified 'alkalic' volume *di–fo–an–CaTs* (Fig. 2), at any pressure. At approximately 25–30 kb, another discontinuity in the liquid trend must occur where the transition between spinel and garnet lherzolite intersects the solidus. Judging from the rate at which the liquid composition trend is approaching the plane *di–fo–an* as pressure increases (Figs. 4 and 5), and the fact that the first melting liquid for garnet lherzolite in this system at 40 kb is in the olivine tholeiite volume (Davis & Schairer, 1965), it appears that this second discontinuity also lies in the olivine tholeiite volume. In more complex systems, it probably lies in the alkalic volume.

## PRODUCTION OF PRIMARY BASALT AT THE CUSP

In the basalt trends shown in Figs. 12 and 13, the atomic ratio $mg = Mg/(Mg + Fe^{2+})$* decreases systematically from a maximum of 0·71† on the left to a minimum of 0·29 on the right. This type of variation occurs within groups of samples from the same locality as well as across the entire composite trend. Also, where data are available, the compositions of olivine phenocrysts show a similar trend of increasing fayalite content to the right. Thus, the least-fractionated basalts are concentrated to the left with the extension to the right being best explained by fractional crystallization involving the removal of olivine, plagioclase, and diopsidic pyroxene (Presnall & O'Donnell, 1976; Clague & Bunch, 1976; Bryan & Moore, 1977).

Assuming that (1) metamorphic peridotites at the base of ophiolite complexes are representative of the residual material remaining after removal of tholeiitic basalts from the mantle, and (2) olivine phenocrysts in mid-ocean ridge basalts are in equilibrium with their host liquid, comparison of olivine compositions in the peridotites with olivine compositions in the least-fractionated basalts should provide a test of the possibility that these basalts represent primary magmas unaffected by fractional crystallization as they moved upward to the earth's surface. The most magnesian olivines in the FAMOUS basalts have a composition of $Fo_{87}$, with *mg* values of the coexisting liquids being 0·70–0·72 (Hekinian *et al.*, 1976). Based on a $K_D = [(X^{Ol}_{FeO})(X^{liq}_{MgO})]/[(X^{liq}_{FeO})(X^{Ol}_{MgO})]$ of 0·3 for basalt, as recommended by Roeder & Emslie (1970), the olivine composition in equilibrium with liquids having these *mg* values would be $Fo_{88-89}$, which supports the assumption that the olivine and host liquid are in equilibrium. Frey *et al.* (1974) reported three analyses of oceanic tholeiites that they considered to be likely candidates for primary magmas. These basalts have compositions (*mg* values are 0·70–0·71) very similar to the least-fractionated FAMOUS basalts and contain olivine phenocrysts that are slightly more forsteritic ($Fo_{90}$), but still within 1–2 per cent Fo of the composition expected from a $K_D$ of 0·3.

Except for one point at $Fo_{84}$, Coleman (1977, Fig. 5) shows the range of olivine compositions in metamorphic peridotites from ophiolites to range from $Fo_{87}$ to $Fo_{94}$, with the main concentration falling in the range $Fo_{90-92}$. Thus, the most magnesian olivines from mid-ocean ridge tholeiites fall within the composition

* For *mg* values of basaltic glasses analyzed with an electron microprobe, it will be assumed throughout that $Fe^{2+}/(Fe^{2+} + Fe^{3+}) = 0·86$.

† One partial analysis listed by Hekinian *et al.* (1976, table 4) has an *mg* value of 0·72.

range of olivines from metamorphic peridotites in ophiolites, but slightly on the iron-rich side of this range. This suggests that mid-ocean ridge tholeiites with *mg* values of 0·70–0·72 are either derived directly from their mantle source and erupted at the earth's surface in an essentially unfractionated condition or have fractionated only a very small amount corresponding to a change in olivine composition of about 2–3 mole per cent Fo.

The three analyses reported by Frey *et al.* (1974) plot, as would be expected from their *mg* values and magnesian olivines, in the left hand portion of the trend shown in Figs. 12 and 13 (points *f7*, *f9*, and *f10*) but it will be noted that they do not all plot in the *extreme* left-hand portion, a result that seems inconsistent with their apparently unfractionated character. It is possible to explain the apparent inconsistency as the result of surprisingly small variations in $Na_2O$ and $SiO_2$, perhaps resulting from sample variation, analytical uncertainties, or both. To illustrate this effect, we have calculated the change in the norm of point *f10* (Figs. 12 and 13) caused by adding 0·4 wt. per cent $NA_2O$ to the listed composition while fixing the amounts of all the other oxides. The resulting norm is shown as *f10'* in Figs. 12 and 13. Not only is the position of the point sensitive to small variations in $Na_2O$ but the shift is approximately along the trend attributed above to fractional crystallization. The norm is much less sensitive to similar variations in the other oxides, but because $SiO_2$ is present in the largest concentration, it usually has the largest absolute uncertainty in a microprobe analysis*. Variations in $SiO_2$ have nearly the same effect on the norm as variations in $Na_2O$ except that a change of one per cent $SiO_2$ (absolute) causes about half the shift produced by a change of 0·4 per cent $Na_2O$. Thus, part of the 'fractionation trend' may be due to small analytical and sampling variations in $NA_2O$. In fact, it is commonly observed that different samples from the same dredge haul (O'Donnell, 1974) or submarine sampling locality (Bryan & Moore, 1977) have nearly identical *mg* values but are dispersed along the 'fractionation trend'. Similarly, the three analyses reported by Frey *et al.* (1974) also have nearly identical *mg* values and are dispersed along the 'fractionation trend' (Figs. 12 and 13). Despite this problem, it is apparent that the *general* correlation of *mg* value and olivine composition with position along the trend requires that fractional crystallization be the main cause of the compositional spread.

If the fractionated basalts were deleted, there would remain a tight grouping of the least-fractionated basalts in the left-hand portion of the overall basalt trend shown in Figs. 12 and 13. The existence of such a parental basalt continuously produced in enormous volumes over long periods of time is a feature that appears to be a worldwide characteristic of volcanism at mid-ocean ridges. In the FAMOUS area, the average Mt. Pluto magma (Bryan & Moore, 1977) is representative of the least-fractionated tholeiites with high *mg* values erupted near the center of the rift valley, and it will be noted that this average analysis falls in the left-hand portion of the trend shown in Figs. 12 and 13.

* For basalt glasses from the mid-Atlantic ridge at 25°–29° N, O'Donnell (1974) found a standard deviation error (2 $\sigma$) of multiple spots analyzed by electron microprobe from a single polished section to be 0·2 wt. per cent for $Na_2O$ and 0·6 wt. per cent for $SiO_2$ (absolute).

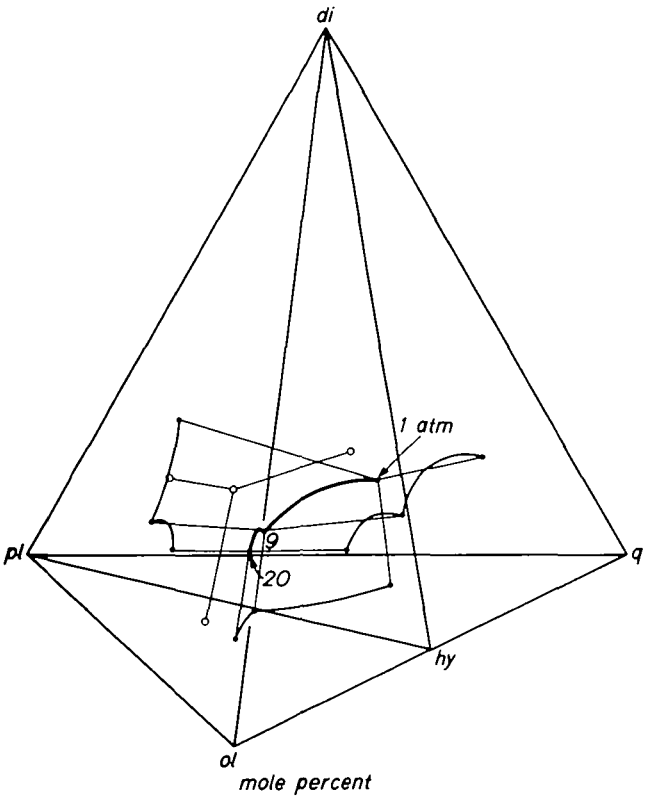


FIG. 15. Perspective drawing of liquid compositions along the solidus curve in Fig. 3 (heavy line with filled circles) and the average Mt. Pluto magma from the FAMOUS area (Bryan & Moore, 1977, open circle). Light solid lines are projections from *pl*, *di*, and *q* onto the faces of the tetrahedron. Numbers indicate pressures in kilobars.

Fig. 15 shows a perspective drawing of the Mt. Pluto average magma and the initial liquid compositions produced along the lherzolite solidus in the system $CaO–MgO–Al_2O_3–SiO_2$ at various pressures. It will be recalled that the addition of other components causes partial melts in equilibrium with lherzolite to shift to higher *di* and *pl* and to lower silica, changes that would shift the composition of the cusp at 9 kb toward the composition of the Mt. Pluto magma. If the magnitude of the effect of additional components is about the same as indicated by Kushiro's (1973) melting experiment on basalt T-87 at 7·5 kb discussed above and shown in Figs. 12, 13, and 14, the match of the 9 kb first liquid composition with the least-fractionated magma is very close. Based on this compositional correspondence, the close correlation of the compositions of olivine phenocrysts from mid-ocean ridge tholeiites and metamorphic peridotites from ophiolites, and the fact that the geotherm is most likely to intersect the solidus at the 9 kb cusp, it is suggested that the parental least-fractionated mid-ocean ridge basalts have been modified very little by fractional crystallization as they passed upward to the surface, and correspond closely to primary melts separated from the source region (rising limb of a convection cell) at about 9 kb.

Irvine (1977) calculated a primitive abyssal tholeiite based on the assumption of

(1) extensive olivine and chromite fractionation prior to the crystallization of other phases and (2) an assumed olivine composition of $Fo_{90.5}$ in equilibrium with this primitive tholeiite. Irvine's primitive liquid (point *i* in Figs. 12, 13, and 14) is picritic and lies toward olivine distinctly separated from the field of analyzed tholeiitic glasses. It will be recalled that the tholeiitic glasses reported by Frey *et al.* (1974) contain olivine phenocrysts with a composition of $Fo_{90}$, yet they are not picritic and plot along the trend of mid-ocean ridge tholeiites (points *f7*, *f9*, and *f10* in Figs. 12 and 13). The direct evidence of Frey *et al.* (1974) on the composition of basalt liquid in equilibrium with olivine having a composition of $Fo_{90}$ is preferred here to the calculation of Irvine (1977). Among abyssal tholeiites that have been reported so far, we are not aware of any *glass* analyses that show a picritic trend toward olivine.

O'Hara (1968*b*) suggested that mid-ocean ridge basalts are generated at 25–30 kb as picritic basalts with their observed compositions at the surface being the result of extensive olivine fractionation as they passed upward to the surface. However, as we have noted, no record of a fractionation trend extending away from the olivine apex is preserved in the glass compositions. Furthermore, none of O'Hara's arguments in favor of fractional crystallization require that it must take place at pressures between 9 and 30 kb. In the absence of any evidence for olivine fractionation at such high pressures, it is more reasonable to conclude that it never occurred, particularly since a mechanism now exists for producing the required parental magma at the 9 kb solidus cusp.

O'Hara (1968*b*, p. 685) assumed that if mid-ocean ridge basalts are derived as primary magmas at about 30 km, the geotherm would lie above the mantle solidus at greater depths near 100 km where picritic primary magmas would be produced. That is, if primary magmas are generated at low pressures, he argued that they must also be produced at higher pressures. However, if the mantle solidus has a cusp at about 9 kb, there is no necessity for the high-pressure portion of the geotherm to be at a higher temperature than the solidus. In fact, the reverse would be expected. In Fig. 16, the range of slopes for the geotherm at mid-ocean ridge crests calculated by various authors from heat flow data is shown as the shaded area. The exact shape of the geotherm at higher pressures is uncertain, but it is clear from the near-surface gradient based on heat-flow measurements that the geotherm must meet the solidus curve at a very shallow depth. The dashed portion of the geotherm is a hypothetical extrapolation, but illustrates the point that basalts could be generated at about 9 kb with no reason to expect, in addition, the generation of picritic basalts at 25–30 kb. The shape of the geotherm will be discussed further in a later section.

O'Hara's (1968*b*) main argument against deriving abyssal tholeiites as primary melts at shallow depths was his contention that compositions of these basalts do not touch the primary phase field of orthopyroxene at any pressure. Thus, he argued that these basalts could not represent unmodified primary magmas derived from a mantle containing olivine and orthopyroxene. It is clear from the above discussion that O'Hara's assumption about the location of the orthopyroxene field is incorrect. The available data indicate that the orthopyroxene field does indeed

touch the compositions of the *least fractionated* mid-ocean ridge tholeiites over a narrow pressure range in the vicinity of 9 kb.

O'Hara (1973) cited the results of Kushiro & Thompson (1972) as experimental verification of his assertion about the location of the orthopyroxene field. Kushiro and Thompson reported a Ca-poor pyroxene at the liquidus of the mid-ocean ridge basalt T-87 over a narrow pressure range at about 7·5 kb, but O'Hara (1973) referred to this pyroxene as a pigeonite (Kushiro and Thompson stated that it was 'most probably orthopyroxene', although it contained 8·9 mole per cent $CaSiO_3$). O'Hara considered it to have a composition more iron rich than residual upper mantle enstatites, which is correct. The *mg* value for residual enstatites from mantle nodules ranges as high as 0·92 for highly depleted mantle and as low as 0·88 for undepleted mantle (Carter, 1970), whereas the pigeonite(?) in the 7·5 kb experiment of Kushiro and Thompson has an *mg* value of 0·84. However the *mg* value of the basaltic liquid in equilibrium with this pigeonite(?) is 0·61 compared to 0·70 for the Mt. Pluto magma of Bryan & Moore (1977), and it is reasonable to infer that if Kushiro and Thompson had carried out their study on a less fractionated basalt like the Mt. Pluto magma, the Ca-poor pyroxene would have also contained less Fe, comparable to the amount inferred by Carter for residual enstatites in nodules. Thus, the experiments of Kushiro and Thompson cannot be considered as verification of O'Hara's position.

A later experiment on another Fe-rich oceanic tholeiite (*mg* value = 0·61) by Fujii & Kushiro (1977) yielded enstatite at the liquidus at 8 kb with an *mg* value estimated by them to be 0·86. This further strengthens the argument that enstatite of an appropriate mantle composition can be in equilibrium with mid-ocean ridge basaltic compositions at about 9 kb.

## AMOUNT OF FUSION AT THE CUSP AND EFFECTS OF MANTLE HETEROGENEITY

At constant pressure, fusion at the simplified lherzolite solidus (Fig. 3) occurs at a quaternary invariant point, which allows the amount of fusion to vary over wide limits without changing the composition of the melt (Presnall, 1969). One method of determining these limits would be to specify the starting composition. Then one could calculate the amount of melt produced just as the crystal path intersected a side, an edge, or a corner of the tetrahedron describing the four crystalline phases (*ol* + *en* + *di* + *sp* or *ol* + *en* + *di* + *an*) in equilibrium with the melt. At this point in the fusion process, one or more of the crystalline phases would be completely consumed and the composition of the liquid would leave the invariant point.

A different procedure will be followed here in order to avoid assumptions about the relative proportions of phases in the starting composition. The composition of the crystalline residue remaining just as fusion at the invariant point is complete will be assumed, and the starting composition will be allowed to slide along the line between the composition of this crystalline residue and the liquid composition at the invariant point. In the pressure range studied here, simplified plagioclase and spinel lherzolites always melt at a peritectic point. Thus, the line between the liquid composition and the bulk composition of the chosen residue would be only

partially contained by the tetrahedron defined by the four crystalline phases in equilibrium with the liquid. Because the starting composition consists of all four crystalline phases, it could slide along the line between the residue and liquid compositions only as long as it remained within the tetrahedron defined by these four crystalline phases. The maximum amount of melt would be obtained for a starting composition situated on the crystalline residue-liquid line just at the point where this line passes out of the tetrahedron.

TABLE 3

*Compositions of phases in equilibrium at 9 kb, 1300 °C invariant point, in weight per cent**

| | *Diopside*† | *Enstatite*† | *Forsterite*† | *Liquid*‡ |
|---|---|---|---|---|
| $SiO_2$ | 51·86 | 55·19 | 42·53 | 49·65 |
| $Al_2O_3$ | 7·70 | 7·50 | — | 20·68 |
| MgO | 20·35 | 35·25 | 57·07 | 14·05 |
| CaO | 20·08 | 2·06 | 0·40 | 15·61 |

* Spinel and anorthite are assumed to be stoichiometric and are therefore not listed.

† Based on unpublished data of J. R. Dixon and Presnall.

‡ Estimated from data in Table 2.

Based on the data of Carter (1970) for ultramafic nodules at Kilbourne's Hole, New Mexico, it will be assumed that fusion at the 9 kb cusp results in the simultaneous depletion of spinel and diopside and leaves a crystalline residue consisting of 87 per cent forsterite, 13 per cent enstatite by weight. Given the composition of the crystalline residue and the phases in equilibrium at the cusp (Table 3), the maximum proportion of liquid that can be extracted from a source capable of being expressed in both of the simplified lherzolite volumes *fo* + *en* + *di* + *an* and *fo* + *en* + *di* + *sp* is calculated by balancing the equation:

crystalline residue (*res*) + liquid (*liq*) = spinel (*sp*) + enstatite (*en*) + diopside (*di*)

This equation is most easily balanced by solving the following determinant (Korzhinskii, 1959, pp. 103–7) expressed in weight fractions:

| | CaO | MgO | $Al_2O_3$ | $SiO_2$ | |
|---|---|---|---|---|---|
| *res* | 0·0062 | 0·5423 | 0·0098 | 0·4417 | |
| *liq* | 0·1561 | 0·1405 | 0·2068 | 0·4965 | |
| *sp* | 0 | 0·2833 | 0·7167 | 0 | = 0 |
| *en* | 0·0206 | 0·3525 | 0·0750 | 0·5519 | |
| *di* | 0·2008 | 0·2035 | 0·0770 | 0·5186 | |

The solution, in weight proportions, is:

$$0{\cdot}00954\ res + 0{\cdot}01957\ liq = 0{\cdot}00301\ sp + 0{\cdot}01180\ en + 0{\cdot}01430\ di \qquad (1)$$

from which the maximum proportion of liquid can be calculated, using the coefficients on the left-hand side of the equation, as 67 per cent. To produce this much liquid of a constant composition at the cusp, the starting composition would

consist of 41 per cent enstatite, 49 per cent diopside, and 10 per cent spinel (the proportion of phases indicated on the right-hand side of equation (1)), with forsterite being absent.

A more realistic approximation of a mantle source composition, this time containing forsterite, can be obtained by sliding the starting composition along the residue-liquid line back toward the crystalline residue composition. For example, if the upper limit on the amount of liquid obtainable at the cusp is reduced to 35 per cent, the proportions of phases in the source material, calculated from equation (1), are 42 per cent forsterite, 27 per cent enstatite, 26 per cent diopside, and 5 per cent spinel. These proportions are considered to be realistic for the mantle, inasmuch as they are essentially identical to those determined by Carter (1970, Table 2A) for an undepleted mantle under Kilbourne's Hole, New Mexico, containing olivine with a composition of $Fo_{86}$.

Other reasonable assumptions about the constitution of the residual material* would yield slightly different results but would not change the basic observation that for realistic model mantle compositions, large variations in the amount of fusion can occur without changing the composition of the initial melt. It should be noted also that considerable heterogeneity in the composition of the source can be tolerated without changing the composition of the initial melt (Yoder & Tilley, 1962, p. 519; Presnall, 1969, pp. 1190–2). It is necessary only that the source composition remain within both of the overlapping tetrahedra forsterite + enstatite + diopside + anorthite and forsterite + enstatite + diopside + spinel, the apices of these tetrahedra being defined by the compositions of the crystalline phases in equilibrium at the cusp.

For actual mantle compositions, fusion would not take place at an invariant point in a rigorous sense because of the presence of small amounts of additional components. Thus, the 9 kb cusp in the simplified system would be expected to correspond, in the mantle, to a low-temperature region spread over a small pressure interval, and some variation in the composition of primary magmas would be expected depending on the composition of the source and the amount of fusion. For example, the *mg* value of liquids would increase as the amount of fusion increases (Presnall, 1969 and in press). The amount of variation in the liquid composition is strongly dependent on the original composition of the source. There are many compositions in simplified systems that do not melt at an invariant point, yet produce liquids that vary in composition only a small amount for large variations in the amount of melting (Presnall, 1969 and in press). For amounts of fusion larger than about 2 per cent, Mysen & Kushiro (1977) have confirmed this type of melting behavior experimentally for natural mantle materials. They found that for lherzolites, an initial temperature interval of about 20–50 °C, in which the initial 1–2 per cent melting takes place, is followed by a second temperature interval of a similar magnitude over which a very large amount of fusion (up to 60 per cent)

* Harzburgite is the most commonly proposed material (for example, see Dickey, 1970; Menzies, 1973; Menzies & Allen, 1974) but the proportions of olivine and orthopyroxene vary somewhat. For example, in metamorphic harzburgites from ophiolites, the proportion of orthopyroxene varies from 5 to 30 volume per cent (Coleman, 1977, p. 25).

occurs without disappearance of any of the major mineral phases. Throughout this second interval, only small changes occur in most of the chemical constituents of the coexisting minerals and liquid. Thus, it would be expected that as mantle material rises in the ascending limb of a convection cell along a mid-ocean ridge, a small amount of fusion, perhaps 1–2 per cent, would occur at depths slightly greater than 30 km, and as the mantle material continues to rise, the amount of fusion would increase sharply at about 30 km, thus facilitating separation of the magma from the source while retaining a fairly constant melt composition.

If magmas at spreading centers are generated at about 30 km depth, the oceanic mantle at depths less than this would be predominantly depleted of its basaltic component whereas at greater depths the basaltic component would be retained (see also Kay *et al.*, 1970; Green, 1972; Oxburgh & Parmentier, 1977). The existence of such a depleted region would explain the rarity of plagioclase lherzolite nodules in oceanic volcanic rocks, for plagioclase lherzolite is stable only at shallow depths (Fig. 3) within the depleted region where the predominant rock type would be residual harzburgite.

## A FIXED POINT ON THE MANTLE GEOTHERM BENEATH OCEANIC RIDGES

In one respect, the model proposed here for the generation of mid-ocean ridge tholeiites is similar to that presented by Green & Ringwood (1967*a*). That is, they suggested 30 km as the depth of magma separation from the source region, about the same depth as proposed here. They considered that fusion starts at a much greater depth*, however, and they attributed the characteristic composition of mid-ocean ridge tholeiites to very rapid upward movement of a mantle diapir such that separation of the melt fraction is delayed until the diapir reaches a depth of about 30 km. They proposed that if the rate of ascent decreases, the depth of magma separation would increase, thereby changing the composition of the separated magma to a low-alumina olivine tholeiite or an alkali olivine basalt. However, such basaltic *liquids* do not exist among any of the volcanic glasses analyzed to date from mid-ocean ridges (Figs. 12, 13, and 14). Schilling & Bonatti (1975) have reported four alkalic analyses of *whole rocks* from the east Pacific Rise, but this ridge is spreading rapidly and would be expected to be accompanied by rapidly rising mantle material. Thus, even if it is considered that these analyses represent liquids, their alkalic character is contrary to the prediction of the Green and Ringwood model.

In the model proposed here, ridges are considered to represent the surface expression of mantle material rising adiabatically over the entire length of the worldwide ridge system; that is, they represent the rising limbs of mantle convection cells. The cusp in the solidus at 9 kb is considered to be the key factor controlling the depth of magma generation and the composition of magma

* In the paper by Green & Ringwood (1967*a*, fig. 12), fusion of an anhydrous diapir rising along an adiabat was indicated as starting at 75–80 km. Later Ringwood (1975, pp. 150–7) modified this model by assuming a mantle with 0·1 wt. per cent water, initiating diapiric rise from about 150 km, and assuming the diapir to be partially liquid throughout its ascent.

produced. The rate of ascent is of subordinate importance. Faster rates of ascent of mantle material would simply result in the production of more lava of a similar composition, whereas a slower rate would decrease the thermal gradient causing a cessation of volcanic activity along the ridge. However, the lowered geothermal gradient would still be high enough to produce incipient fusion in the oceanic seismic low-velocity zone (Presnall, 1978).

It is suggested that the cusp on the mantle solidus acts as a thermal buffer that controls the shape of the geotherm at active mid-ocean ridges. The effect of the heat of fusion combined with separation and ascent of magma at 9 kb from upwardly convecting mantle material would depress the geotherm whereas the geotherm would rise during periods without magma production. The net result would be stabilization of the geotherm just at the cusp, as shown in Fig. 16.

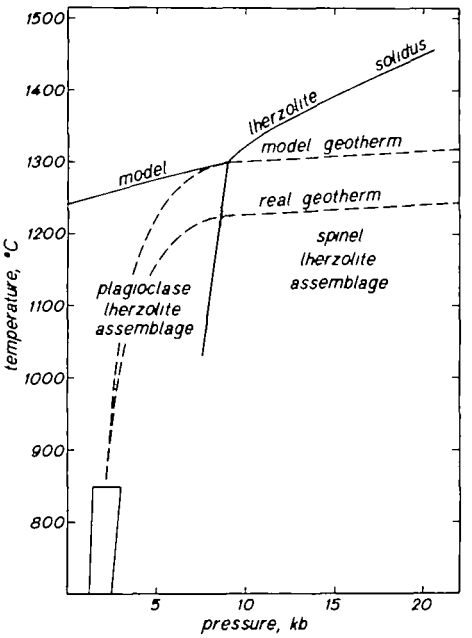


FIG. 16. Simplified lherzolite solidus curve from Fig. 3 and two dashed hypothetical extensions of the geotherm for the mantle beneath mid-ocean ridges, one for the model mantle system $CaO–MgO–Al_2O_3–SiO_2$ and one for the real mantle. The shaded area is the range of slopes calculated by Oxburgh & Turcotte (1968), Le Pichon & Langseth (1970), and Bottinga & Allègre (1973), and the hachured area is the estimated pressure and temperature at which primary tholeiites are generated in the real mantle. The geothermal gradient at pressures above 9 kb is adiabatic (0·5 °C/km).

The model geotherm drawn is for a mature ridge and is adiabatic (0·5 °C/km) at pressures greater than 9 kb. Such a gradient is consistent with the concept of rapid, and therefore essentially adiabatic, convective upwelling of mantle material along ridges, and with the gradient of approximately 1 °C/km determined from magneto-telluric data by Hermance & Grillot (1974) beneath Iceland. For newly-formed ridges, mantle material rising adiabatically might intersect the solidus curve at some pressure higher than 9 kb, but as the ridge matures, the intersection would be expected to migrate to lower pressures and finally stabilize at the cusp. In this case,

the early volcanics would be generated at higher pressures and would tend to be more alkalic in composition. It is interesting to note that this trend is exactly what is observed in the Ethiopian Rift (Gass, 1970; Mohr, 1971), a feature that is presumably an example of a spreading center in its initial stages of formation.

Assuming the cusp corresponds to a fixed point on the geotherm beneath active oceanic ridges, an estimate of the effect of additional components on the temperature and pressure at the cusp would be useful in constructing thermal models for the mantle. For pyrolite, Green & Ringwood (1967*b*) found the solidus temperatures at 9 and 20 kb to be lower than our solidus curve (Fig. 2) by 75 and 65 °C, respectively. Mysen & Kushiro (1977) took the lherzolite 66SAL-1 as representative of the least chemically depleted oceanic mantle. They found that at 20 kb, large amounts of liquid (1·5 to 60 per cent) were produced at 1350–1375 °C, a temperature range 70–95 °C lower than our solidus at 20 kb. From these studies, it appears that our solidus curve is about 50–100 °C higher than temperatures for the occurrence of large amounts of melting in mantle compositions containing additional components. Thus, the mantle equivalent of the cusp in the simplified system would probably occur at about 1200–1250 °C. Because of the large amount of fusion indicated at the cusp, the presence of small amounts of $CO_2$ and $H_2O$ in the mantle would not alter this estimate appreciably.

The effect of additional components on the plagioclase to spinel lherzolite transition, which at high temperatures is essentially the pressure of the cusp, has been studied by Green & Hibberson (1970) and Emslie (1971). Green and Hibberson found the maximum stability of plagioclase in a pyrolite bulk composition to be 11·2 kb. As would be expected in a complex composition, plagioclase and spinel were found to coexist over a range of pressure, but the lower limit of this range was not defined. They listed one run containing both plagioclase and spinel at 4·5 kb and 1200 °C, but it is important to note that their runs in the absence of a liquid phase were a maximum of 4 hours long, far shorter than we have found to be necessary for runs containing a liquid phase. Emslie, using a mixture of natural olivine and plagioclase, found the maximum stability of plagioclase to be 10 kb. No minimum pressure for the coexistence of plagioclase and spinel was determined. Thus, the available data are inconclusive, but suggest that the transition between plagioclase and spinel lherzolite occurs over a range of pressure that is not appreciably displaced from the 9 kb transition found in the system $CaO–MgO–Al_2O_3–SiO_2$.

From the above discussion, it is estimated that the region of magma generation for the real mantle beneath active ridges would be centered at about 9 kb and 1200–1250 °C. Fig. 16 shows this region as the hachured area together with the estimated real geotherm.

## FRACTIONAL VERSUS EQUILIBRIUM FUSION

The constraint imposed by LIL element studies that mid-ocean ridge tholeiites are the result of a large amount of partial fusion (Gast, 1968; Kay *et al.*, 1970; Schilling, 1971, 1975) requires that equilibrium fusion rather than fractional fusion (Presnall, 1969) applies. Langmuir *et al.* (1977) have also shown that a close

approach to fractional fusion, that is, stepwise equilibrium fusion (Presnall, in press) and extraction of melt from the same source in small increments, would produce highly variable La/Yb ratios, which are not observed. However, Schilling (1975) has shown that the observed rare earth element (REE) patterns can be explained by variations in the amount of equilibrium fusion between about 10 and 30 per cent if each basalt sampled is extracted from a fresh source. In agreement with Schilling's conclusion, White & Bryan (1977) calculated for the FAMOUS basalts that the major element differences between the most primitive and most fractionated basalts can be explained by about 23 per cent crystallization, whereas LIL elements (K, Rb, Ba, and REE) are enriched by factors of 2–4. Because 23 per cent crystallization is inadequate to explain these enrichment factors, they invoked varying degrees of equilibrium fusion. Hart *et al.* (1973) have also discussed the inadequacy of fractional crystallization as a mechanism for explaining the LIL element concentrations.

In the FAMOUS area, Langmuir *et al.* (1977) found the additional complication of crossing REE distribution patterns and concluded that one way to explain these results would be to postulate a source with heterogeneous REE distribution patterns. However, they preferred to explain the crossing patterns by invoking a homogeneous source and postulating a combination of at least (1) varying amounts of single-step equilibrium fusion, with each melt extracted from a fresh portion of the source, and (2) stepwise equilibrium fusion in moderately large steps from the same source with retention in the residue of some of the melt produced at each step. In either case, the arguments against a close approach to fractional fusion would hold.

Thus a satisfactory explanation of both the major and trace element data appears to require variations in the amount of equilibrium fusion as well as variations in the amount of subsequent fractional crystallization. Varying amounts of equilibrium fusion (up to a maximum of 35 per cent in our model calculation) would generate primary magmas with fairly uniform major element compositions but widely different LIL element concentrations, whereas subsequent fractional crystallization of these primary magmas would produce most of the observed differences in the major element compositions of the erupted lavas, but would have only a second-order influence on the concentrations of the LIL elements. It would be expected that the resulting partially fused uppermost portion of the oceanic mantle (about 8–30 km depth) would display varying degrees of depletion, as is observed for alpine peridotites believed to be samples of this portion of the mantle (Dick, 1977, p. 827; Richard *et al.*, 1976, p. 272). Wide variations in the amount of equilibrium fusion at the mantle equivalent of the 9 kb cusp would require temperature differences of only 20–50 °C (Mysen & Kushiro, 1977).

## ACKNOWLEDGEMENTS

We wish to thank T. N. Irvine, M. J. O'Hara, and H. S. Yoder, Jr. for critical review of the manuscript. It will be recognized, however, that some of their views deviate strongly from those expressed here. This research was supported by the Earth Sciences Section, National Science Foundation, NSF Grants GA-21477, DES 74-22571, and EAR 74-22571 A01.

## APPENDIX

### *Experimental details*

For the one-atmosphere runs, vertical, platinum-wound quench furnaces (Shepherd *et al.*, 1909) were used. The Pt/Pt10Rh working thermocouples were calibrated by comparison against a standard Pt/Pt10Rh thermocouple certified by the National Bureau of Standards. Mixtures were contained in folded platinum foil envelopes and quenched by dropping them from the hot zone of the furnace into water.

For the high-pressure runs, a solid media, piston-cylinder apparatus was used, and the experimental method is identical to that described by Presnall (1976, p. 583). Also, the method for determining the solidus curve is described by Presnall (1976, pp. 583–4). All temperatures have been adjusted to the 1968 International Practical Temperature Scale (Anonymous, 1969). The uncertainty brackets in Fig. 3 are based on an assumed uncertainty for each run of ±10 °C and ±0·5 kb. These limits are the extremes that have been found by experience to be necessary in order to obtain internally consistent data. Table 4 gives the compositions and CIPW normative mineralogy of the starting mixtures used for the runs listed in Table 1.

TABLE 4

*Compositions and CIPW normative mineralogy (weight per cent) of starting mixtures*

| | *CMAS-3* | *CMAS-5* | *CMAS-6* | *CMAS-7* |
|---|---|---|---|---|
| $SiO_2$ | 50·25 | 48·93 | 48·73 | 50·94 |
| $Al_2O_3$ | 11·83 | 18·26 | 13·56 | 17·59 |
| MgO | 26·70 | 18·92 | 28·14 | 16·35 |
| CaO | 11·23 | 13·89 | 9·57 | 15·12 |
| *an* | 32·28 | 49·82 | 37·00 | 48·00 |
| *di* | 18·24 | 14·86 | 8·16 | 21·00 |
| *en* | 29·47 | 23·81 | 28·01 | 31·00 |
| *fo* | 20·02 | 11·51 | 26·83 | — |

In Fig. 3, the solidus curve was reversed using runs of 6 hours duration at 9·3 and 14 kb (Presnall, 1976, table 2). Based on these results, the other runs bracketing the solidus curve, all at least 24 hours long, are considered to represent equilibrium results. The data points shown in Fig 3 are a combination of some of the 24 hour runs reported earlier (Presnall, 1976) for the portion of this curve between 8 and 14 kb and longer 48 hour runs given in Table 1. Very long run times were utilized because it was found that times required to prove reversibility of the univariant reactions were not adequate for producing phases sufficiently homogeneous for electron microprobe analysis.

To facilitate electron microprobe analyses of the glasses, the compositions of the starting mixtures were chosen so as to produce a large amount of glass for runs along the solidus curve. Typically, runs that were analyzed consisted of 30 to 50 per cent glass, making it possible to check for homogeneity by analyzing the glass in all parts of the charge. Minor amounts of quench crystals were sometimes present, usually as overgrowths on equilibrium crystals, and to check for any effect

of these quench crystals on the glass composition, electron microprobe traverses were made from the margins of quench crystals out into large areas of clear glass. No composition gradients in the glass were observed and it was concluded that the formation of quench crystals did not alter the composition of the glass, except perhaps immediately adjacent to the quench crystals on a scale smaller than the 5 micron diameter analytical volume of the electron beam.

Each of the runs analyzed contained all the phases in equilibrium on the univariant solidus curve. It was possible to make such runs without too much difficulty because of a thermal gradient of about 10 °C inside the platinum sample capsule and small variations in temperature and pressure during the course of a run.

## REFERENCES


ANDERSEN, O., 1915. The system anorthite–forsterite–silica. *Am. J. Sci.* **39** (Fourth Ser.), 407–54.

ANONYMOUS, 1969. The international practical temperature scale of 1968. *Metrologia*, **5**, 35–44.

BELL, P. M., & ROSEBOOM, E. H., JR., 1969. Melting relationships of jadeite and albite to 45 kilobars with comments on melting diagrams of binary systems at high pressures. *Spec. Pap. Mineralog. Soc. Am.* **2**, 151–61.

BOTTINGA, Y., & ALLÈGRE, C. J., 1973. Thermal aspects of sea-floor spreading and the nature of the oceanic crust. *Tectonophysics*, **18**, 1–17.

BOWEN, N. L., 1914. The ternary system diopside–forsterite–silica. *Am. J. Sci.* **38** (Fourth Ser.), 207–64.

BOYD, F. R., ENGLAND, J. L., & DAVIS, B. T. C., 1964. Effects of pressure on the melting and polymorphism of enstatite, $MgSiO_3$. *J. geophys. Res.* **69**, 2101–9.

BRYAN, W. B., & MOORE, J. G., 1977. Compositional variations of young basalts in the Mid-Atlantic Ridge rift valley near lat. 36°49′ N. *Bull. geol. Soc. Am.* **88**, 556–70.

CARTER, J. L., 1970. Mineralogy and chemistry of the earth's upper mantle based on the partial fusion–partial crystallization model. *Ibid.* **81**, 2021–34.

CHEN, C.-H., & PRESNALL, D. C., 1975. The system $Mg_2SiO_4$–$SiO_2$ at pressures up to 25 kilobars. *Am. Miner.* **60**, 398–406.

CLAGUE, D. A., & BUNCH, T. E., 1976. Formation of ferrobasalt at east Pacific midocean spreading centers. *J. geophys. Res.* **81**, 4247–56.

CLARK, S. P., JR., SCHAIRER, J. F., & DE NEUFVILLE, J., 1962. Phase relations in the system $CaMgSi_2O_6$–$CaAl_2SiO_6$–$SiO_2$ at low and high pressure. *Yb. Carnegie Instn. Wash.* **61**, 59–68.

COLEMAN, R. G., 1977. *Ophiolites*, Springer-Verlag.

DAVIS, B. T. C., & SCHAIRER, J. F., 1965. Melting relations in the join diopside–forsterite–pyrope at 40 kilobars and at one atmosphere. *Yb. Carnegie Instn. Wash.* **64**, 123–6.

DELANEY, J. R., MEUNOW, D., & GRAHAM, D. G. (in press). Abundance and distribution of water, carbon and sulfur in the glassy rims of submarine pillow basalts. *Geochim. cosmochim. Acta.*

DICK, H. J. B., 1977. Partial melting in the Josephine peridotite I, the effect on mineral composition and its consequence for geobarometry and geothermometry. *Am. J. Sci.* **277**, 801–32.

DICKEY, J. S., JR., 1970. Partial fusion products in alpine-type peridotites: Serrania de la Ronda and other examples. *Spec. Pap. Mineralog. Soc. Am.* **3**, 33–49.

EGGLER, D. H., 1974. Effect of $CO_2$ on the melting of peridotite. *Yb. Carnegie Instn. Wash.* **73**, 215–24.

—— 1975. Peridotite–carbonate relations in the system $CaO$–$MgO$–$SiO_2$–$CO_2$. Ibid. **74**, 468–74.

—— 1976. Does $CO_2$ cause partial melting in the low-velocity layer of the mantle? *Geology*, **4**, 69–72.

EMSLIE, R. F., 1971. Liquidus relations and subsolidus reactions in some plagioclase-bearing systems. *Yb. Carnegie Instn. Wash.* **69**, 148–55.

ENGEL, A. E. J., & ENGEL, C. G., 1964. Composition of basalts from the Mid-Atlantic Ridge. *Science*, **144**, 1–4.

—— —— & HAVENS, R. G., 1965. Chemical characteristics of oceanic basalts and the upper mantle. *Bull. geol. Soc. Am.* **76**, 719–34.

FREY, F. A., BRYAN, W. B., & THOMPSON, G., 1974. Atlantic Ocean floor: geochemistry and petrology of basalts from legs 2 and 3 of the Deep Sea Drilling Project. *J. geophys. Res.* **79**, 5507–27.

FUJII, T., & KUSHIRO, I., 1977. Melting relations and viscosity of an abyssal tholeiite. *Yb. Carnegie Instn. Wash.* **76**, 461–5.

GASS, I. G., 1970. The evolution of volcanism in the junction area of the Red Sea, Gulf of Aden and Ethiopian rifts. *Phil. Trans. R. Soc. Lond.* **A 267**, 369–81.

GAST, P. W., 1968. Trace element fractionation and the origin of tholeiitic and alkaline magma types. *Geochim. cosmochim. Acta*, **32**, 1057–86.

GREEN, D. H., 1972. Composition of basaltic magmas as indicators of conditions of origin: application to oceanic volcanism. *Phil. Trans. R. Soc. Lond.* **A 268**, 707–25.

—— & HIBBERSON, W., 1970. The instability of plagioclase in peridotite at high pressures. *Lithos*, **3**, 209–21.

—— & RINGWOOD, A. E., 1967*a*. The genesis of basaltic magmas. *Contr. Miner. Petrol.* **15**, 103–90.

—— —— 1967*b*. The stability fields of aluminous pyroxene peridotite and garnet peridotite and their relevance in upper mantle structure. *Earth planet Sci. Lett.* **3**, 151–60.

HAMILTON, D. L., BURNHAM, C. W., & OSBORN, E. F., 1964. The solubility of water and effects of oxygen fugacity and water content on crystallization in mafic magmas. *J. Petrology*, **5**, 21–39.

HART, S. R., & NALWALK, A. J., 1970. K, Rb, Cs and Sr relationships in submarine basalts from the Puerto Rico trench. *Geochim. cosmochim. Acta* **34**, 145–55.

—— SCHILLING, J.-G., & POWELL, J. L., 1973. Basalts from Iceland and along the Reykjanes Ridge: Sr isotope geochemistry. *Nature Phys. Sci.* **246**, 104–7.

HEKINIAN, R., MOORE, J. G., & BRYAN, W. B., 1976. Volcanic rocks and processes of the Mid-Atlantic Ridge rift valley near 36°49′ N. *Contr. Miner. Petrol.* **58**, 83–110.

HERMANCE, J. F., & GRILLOT, L. R., 1974. Constraints on temperature beneath Iceland from magnetotelluric data. *Phys. Earth planet. Interiors* **8**, 1–12.

HERZBERG, C. T., 1972. Stability fields of plagioclase- and spinel-lherzolite. *Prog. Exp. Petrology*, Nat. Environ. Res. Council, **2**, 145–8.

—— & O'HARA, M. J., 1972. Temperature and pressure calibration and reproducibility of pressure in solid media equipment. *Ibid.* **2**, 98–8.

HYTÖNEN, K., & SCHAIRER, J. F., 1960. The system enstatite–anorthite–diopside. *Yb. Carnegie Instn. Wash.* **59**, 71–2.

IRVINE, T. N., 1977. Definition of primitive liquid compositions for basic magmas. *Ibid.* **76**, 454–61.

KAY, R., HUBBARD, N. J., & GAST, P. W., 1970. Chemical characteristics and origin of oceanic ridge volcanic rocks. *J. geophys. Res.* **75**, 1585–1613.

KORZHINSKII, D. S., 1959. *Physicochemical basis of the analysis of the paragenesis of minerals*. New York: Consultants Bureau.

KUSHIRO, I., 1968. Compositions of magmas formed by partial zone melting of the earth's upper mantle. *J. geophys. Res.* **73**, 619–34.

—— 1969. The system forsterite–diopside–silica with and without water at high pressures. *Am. J. Sci.* **267A**, 269–94.

—— 1972*a*. Effect of water on the composition of magmas formed at high pressures. *J. Petrology*, **13**, 311–34.

—— 1972*b*. Determination of liquidus relations in synthetic silicate systems with electron probe analysis: the system forsterite–diopside–silica at 1 atmosphere. *Am. Miner.* **57**, 1260–71.

—— 1972*c*. Partial melting of synthetic and natural peridotites at high pressures. *Yb. Carnegie Instn. Wash.* **71**, 357–62.

—— 1973. Origin of some magmas in oceanic and circum-oceanic regions. *Tectonophysics*, **17**, 211–22.

—— & THOMPSON, R. N., 1972. Origin of some abyssal tholeiites from the Mid-Atlantic Ridge. *Yb. Carnegie Instn. Wash.* **71**, 403–6.

—— & YODER, H. S., JR., 1965. The reactions between forsterite and anorthite at high pressures. *Ibid.* **64**, 89–94.

—— —— 1966. Anorthite–forsterite and anorthite–enstatite reactions and their bearing on the basalt–eclogite transformation. *J. Petrology*, **7**, 337–62.

—— —— & NISHIKAWA, M., 1968. Effect of water on the melting of enstatite. *Bull. geol. Soc. Am.* **79**, 1685–92.

LAMBERT, I. B., & WYLLIE, P. J., 1970*a*. Low-velocity zone of the earth's mantle: incipient melting caused by water. *Science*, **169**, 764–6.

—— —— 1970*b*. Melting in the deep crust and upper mantle and the nature of the low velocity layer. *Phys. Earth planet. Interiors*, **3**, 316–22.

LANGMUIR, C. H., BENDER, J. F., BENCE, A. E., HANSON, G. N., & TAYLOR, S. R., 1977. Petrogenesis of basalts from the FAMOUS area: Mid-Atlantic Ridge. *Earth planet. Sci. Lett.* **36**, 133–56.

LEPICHON, X., & LANGSETH, M. G., JR., 1970. Heat flow from the mid-ocean ridges and sea-floor spreading. *Tectonophysics*, **8**, 319–44.

MACGREGOR, I. D., 1965. Stability fields of spinel and garnet peridotites in the synthetic system $MgO$–$CaO$–$Al_2O_3$–$SiO_2$. *Yb. Carnegie Instn. Wash.* **64**, 126–34.

MELSON, W. G., BYERLY, G. R., NELEN, J. A., O'HEARN, T., WRIGHT, T. L., & VALLIER, T., 1976. A catalog of the major element chemistry of abyssal volcanic glasses. In MASON, B. (ed.), *Mineral Sciences Investigations, 1974–1975, Smithsonian Contrib. Earth Sciences*, **19**, 31–60.

—— & THOMPSON, G., 1971. Petrology of a transform fault zone and adjacent ridge segments. *Phil. Trans. R. Soc. Lond.* **A 268**, 423–41.

MENZIES, M. A., 1973. Mineralogy and partial melt textures within an ultramafic–mafic body, Greece. *Contr. Miner. Petrol.* **42**, 273–85.

—— & ALLEN, C., 1974. Plagioclase lherzolite-residual mantle relationships within two eastern Mediterranean ophiolites. *Ibid.* **45**, 197–213.

MIYASHIRO, A., SHIDO, F., & EWING, M., 1969. Diversity and origin of abyssal tholeiite from the Mid-Atlantic Ridge near 24° and 30° north latitude. *Ibid.* **23**, 38–52.

MOHR, P. A., 1971. Ethiopian Rift and plateaus: some volcanic petrochemical differences. *J. geophys. Res.* **76**, 1967–84.

MOORE, J. G., 1970. Water content of basalt erupted on the ocean floor. *Contr. Miner. Petrol.* **28**, 272–9.

MYSEN, B. O., & BOETTCHER, A. L., 1975. Melting of a hydrous mantle: II. Geochemistry of crystals and liquids formed by anatexis of mantle peridotite at high pressures and high temperatures as a function of controlled activities of water, hydrogen, and carbon dioxide. *J. Petrology*, **16**, 549–93.

—— & KUSHIRO, I., 1977. Compositional variations of coexisting phases with degree of melting of peridotite in the upper mantle. *Am. Miner.* **62**, 843–65.

O'DONNELL, T. H., 1974. Chemical and petrographic features of basalts from 25°–29° N on the Mid-Atlantic ridge. *Unpub. M.S. Thesis, The Univ. Texas at Dallas.*

O'HARA, M. J., 1965. Primary magmas and the origin of basalts. *Scot. J. Geol.* **1**, 19–40.

—— 1968*a*. The bearing of phase equilibria studies in synthetic and natural systems on the origin and evolution of basic and ultrabasic rocks. *Earth Sci. Revs.* **4**, 69–133.

—— 1968*b*. Are ocean floor basalts primary magma? *Nature*, **220**, 683–6.

—— 1973. Non-primary magmas and dubious mantle plume beneath Iceland. *Ibid.* **243**, 507–8.

—— RICHARDSON, S., & WILSON, G., 1971. Garnet-peridotite stability and occurrence in crust and mantle. *Contr. Miner. Petrol.* **32**, 48–68.

OSBORN, E. F., & TAIT, D. B., 1952. The system diopside–forsterite–anorthite. *Am. J. Sci. Bowen Vol.*, 413–33.

OXBURGH, E. R., & PARMENTIER, E. M., 1977. Compositional and density stratification in oceanic lithosphere—causes and consequences. *J. geol. Soc. Lond.* **133**, 343–55.

—— & TURCOTTE, D. L., 1968. Mid-ocean ridges and geotherm distribution during mantle convection. *J. geophys. Res.* **73**, 2643–61.

PRESNALL, D. C., 1969. The geometrical analysis of partial fusion. *Am. J. Sci.* **267**, 1178–94.

—— 1976. Alumina content of enstatite as a geobarometer for plagioclase and spinel lherzolites. *Am. Miner.* **61**, 582–8.

—— 1978. A double seismic low-velocity zone beneath mid-oceanic ridges. *Trans. Am. geophys. Un.* **59**, 369–70 (abstr.).

—— (in press.) Fractional crystallization and partial fusion. In YODER, H. S., JR. (ed.), *The Evolution of the Igneous Rocks: A Fiftieth Anniversary Perspective.* Princeton: Princeton University Press.

—— DIXON, S. A., DIXON, J. R., O'DONNELL, T. H., BRENNER, N. L., SCHROCK, R. L., & DYCUS, D. W., 1978. Liquidus phase relations on the join diopside–forsterite–anorthite from 1 atm to 20 kbar: Their bearing on the generation and crystallization of basaltic magma. *Contr. Miner. Petrol.* **66**, 203–20.

—— & O'DONNELL, T. H., 1976. Origin of basalts from 25°–29° N on the Mid-Atlantic ridge. *Trans. Am. geophys. Un.* **57**, 341 (abstr.).

RICHARD, P., SHIMIZU, N., & ALLÈGRE, C. J., 1976. $^{143}Nd/^{146}Nd$, a natural tracer: an application to oceanic basalts. *Earth planet Sci. Lett.* **31**, 269–78.

RINGWOOD, A. E., 1975. *Composition and petrology of the earth's mantle.* New York: McGraw-Hill.

ROEDDER, E., 1965. Liquid $CO_2$ inclusions in olivine-bearing nodules and phenocrysts from basalts. *Am. Miner.* **50**, 1746–82.

ROEDDER, E., 1965. Liquid $CO_2$ inclusions in olivine-bearing nodules and phenocrysts from basalts. *Am. Miner.* **50**, 1746–82.

ROEDER, P. L., & EMSLIE, R. F., 1970. Olivine-liquid equilibrium. *Contr. Miner. Petrol.* **29**, 275–89.

SCHILLING, J.-G., 1971. Sea-floor evolution: rare-earth evidence. *Phil. Trans. R. Soc. Lond.* A **268**, 663–706.

—— 1975. Rare-earth variations across 'normal segments' of the Reykjanes Ridge, 60°–53° N, Mid-Atlantic Ridge, 29° S, and East Pacific Rise, 2°–19° S, and evidence on the composition of the underlying low-velocity layer. *J. geophys. Res.* **80**, 1459–73.

—— & BONATTI, E., 1975. East Pacific Ridge (2° S–19° S) versus Nazca intraplate volcanism: rare-earth evidence. *Earth planet Sci. Lett.* **25**, 93–102.

SCHREINEMAKERS, F. A. H., 1915*a*. In-, mono-, and di-variant equilibria. I. *Proc. Sect. Sci. K. ned. Akad. Wet.* **18**, 116–26.

—— 1915*b*. In-, mono-, and di-variant equilibria II. *Ibid.* **18**, 531–42.

—— 1915*c*. In-, mono-, and di-variant equilibria III. *Ibid.* **18**, 820–8.

SHEPHERD, E. S., RANKIN, G. A., & WRIGHT, F. E., 1909. The binary systems of alumina with silica, lime, and magnesia. *Am. J. Sci.* **28** (Fourth Ser.), 293–333.

SHIBATA, T., 1975. Crystallization of abyssal tholeiites. *Trans. Am. geophys. Un.* **56**, 468 (abstr.).

SHIDO, F., MIYASHIRO, A., & EWING, M., 1971. Crystallization of abyssal tholeiites. *Contr. Miner. Petrol.* **31**, 251–66.

WHITE, W. M., & BRYAN, W. B., 1977. Sr-isotope, K, Rb, Cs, Sr, Ba and rare-earth geochemistry of basalts from the FAMOUS area. *Bull. geol. Soc. Am.* **88**, 571–6.

WYLLIE, P. J., & HUANG, W.-L., 1975. Influence of mantle $CO_2$ in the generation of carbonatites and kimberlites. *Nature*, **257**, 297–9.

YANG, H.-Y., 1973. Crystallization of iron-free pigeonite in the system anorthite–diopside–enstatite–silica at atmospheric pressure. *Am. J. Sci.* **273**, 488–97.

YODER, H. S., JR., & TILLEY, C. E., 1962. Origin of basalt magmas: an experimental study of natural and synthetic rock systems. *J. Petrology*, **3**, 342–532.